Photoneutron cross section measurements with laser Compton-scattering γ-ray beams

Hiroaki Utsunomiya

(Konan University, CNS University of Tokyo)

Content

1. γ-ray sources
   Positron annihilation in flight vs laser inverse Compton scattering
2. Photoneutron measurements
   a. E1 (pygmy dipole resonance) and M1 cross sections
   b. Applications of the reciprocity theorem
   c. p-process nucleosynthesis
   d. γ-ray strength function for (n,g) c.s. for radioactive nuclei

September 15 & 16, 2014
Lomonosov Moscow State University (MSU)
Skobeltsyn Institute of Nuclear Physics (SINP)
Department of Electromagnetic Processes and Atomic Nuclei Interactions (DEPANI)

γ-ray sources: Positron annihilation in flight

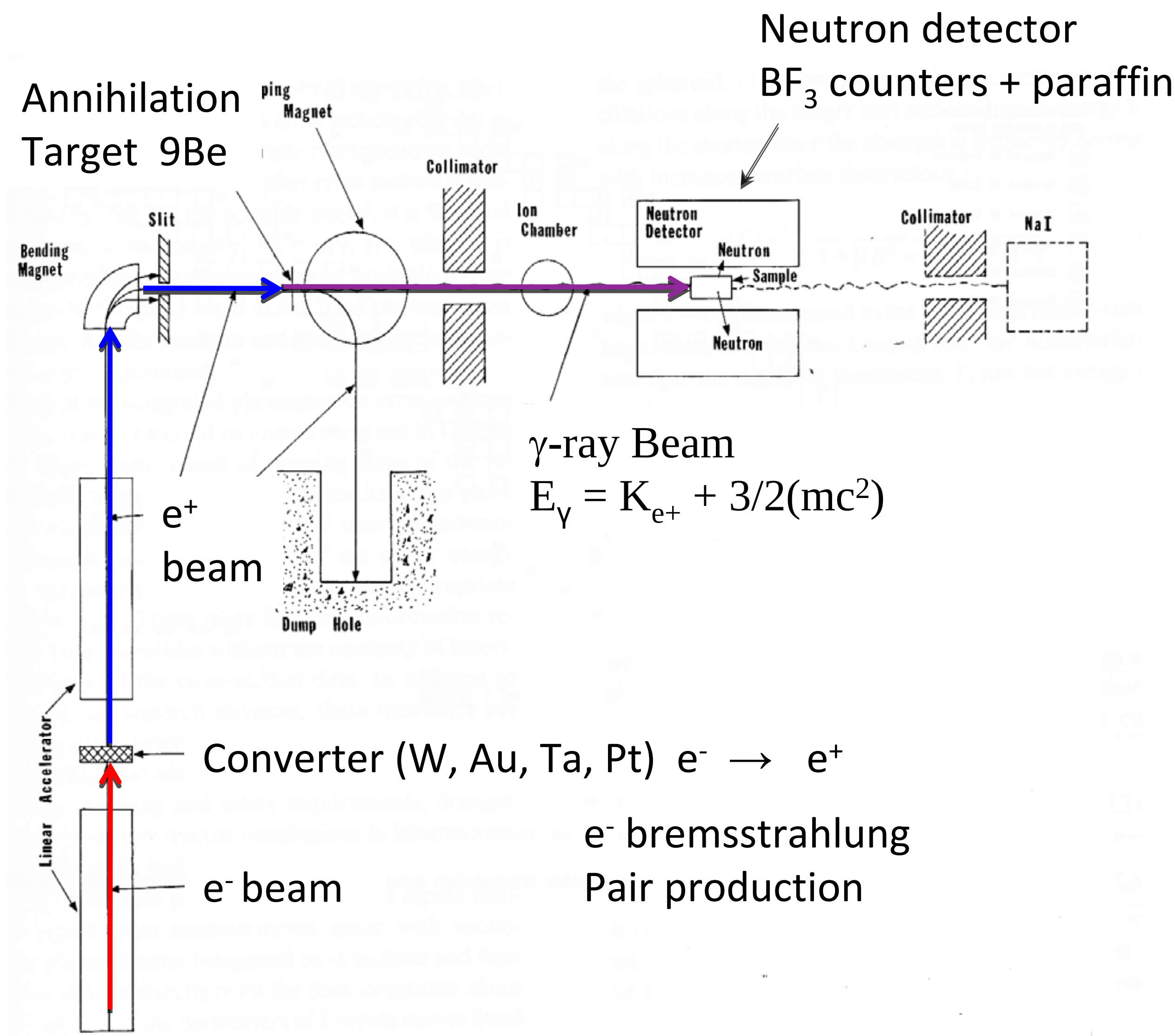

Lawrence Livermore National Laboratory (USA)

Saclay (France)

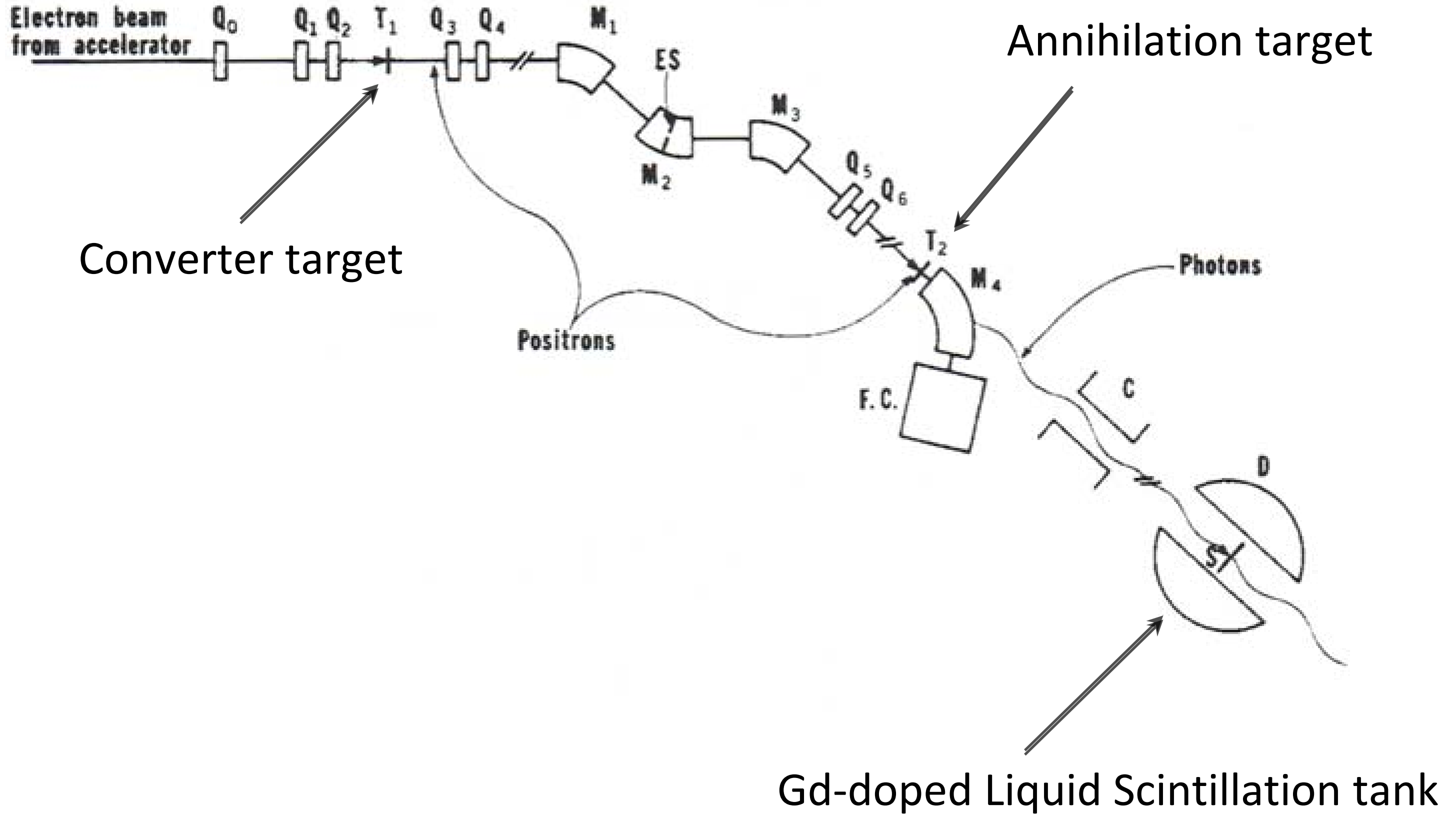

e^+-e^- annihilation
(quasi-monochromatic)

Subtracted

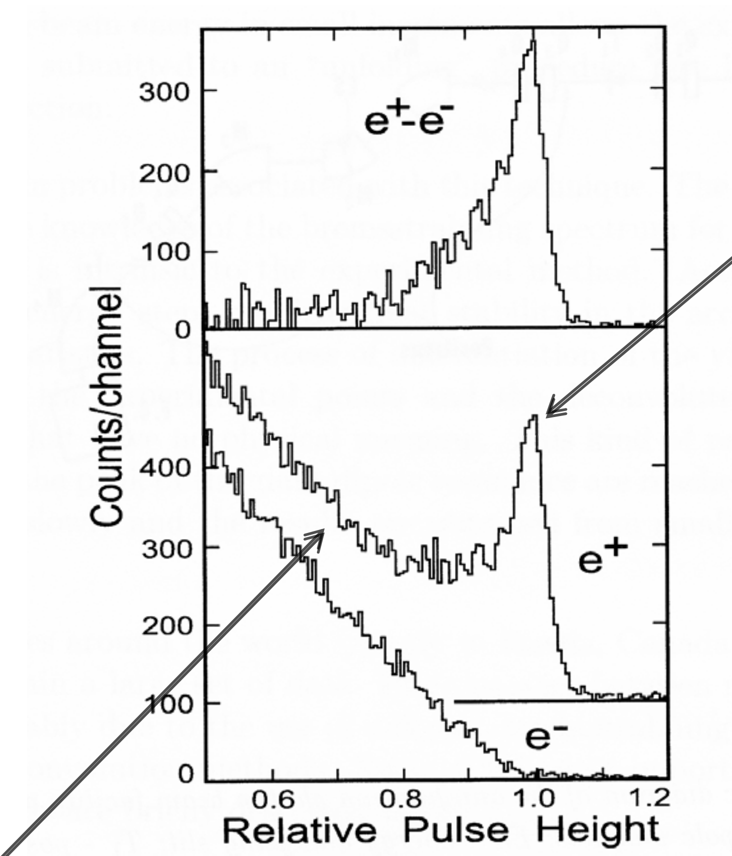

e^+ bremsstrahlung
(background)

γ-ray sources: Inverse Compton scattering

Compton scattering vs Inverse Compton scattering

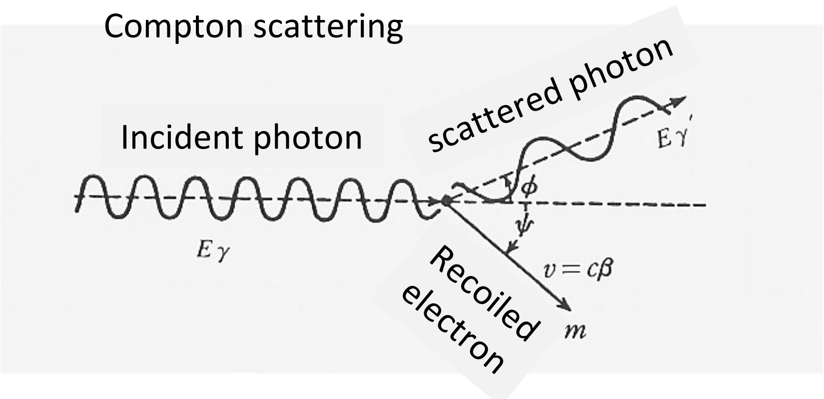

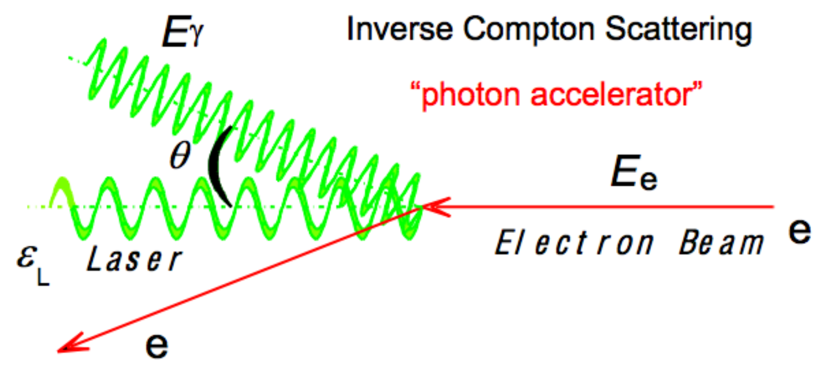

$$h\nu' = \frac{h\nu}{1 + h\nu(1-\cos\phi)/mc^2}$$

$$h\nu + mc^2 = h\nu' + \sqrt{p^2c^2 + m^2c^4}$$

$$\frac{h\nu}{c} = \frac{h\nu'}{c}\cos\phi + p\cos\psi$$

$$0 = \frac{h\nu'}{c}\sin\phi - p\sin\psi$$

$$E_\gamma = \frac{4\gamma^2\varepsilon_L}{1 + (\gamma\theta)^2 + 4\gamma\varepsilon_L/(mc^2)}$$

$\gamma = E_e/mc^2$ Lorentz factor

Laser Compton scattering γ-ray beam

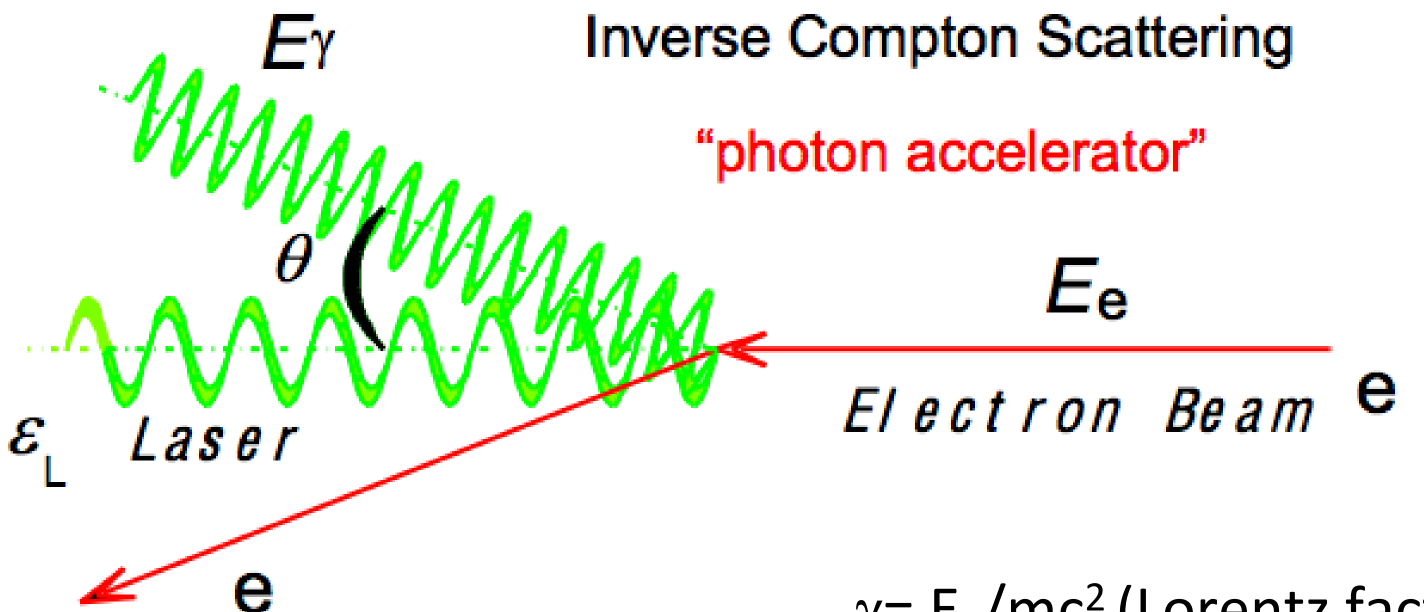

$$E_\gamma = \frac{4\gamma^2\varepsilon_L}{1 + (\gamma\theta)^2 + 4\gamma\varepsilon_L/(mc^2)}$$

$$\Delta E/E \cong \left\{\left(\frac{2\Delta E_e}{E_e}\right)^2 + \gamma^4(\theta_e^2 + \theta_c^2)^2\right\}^{1/2}$$

$\gamma = E_e/mc^2$ (Lorentz factor)

□ 2×10^3 E_e=1 GeV

Energy am

$E_\gamma/\varepsilon_L = 4\gamma^2$□$1.6 \times 10^7$

ε_L□ 1eV

E_γ □ 16 MeV


LEPS, LEPS2
GeV γ
SPring8 8 GeV e- storage ring
SACLA
8 GeV e- linac
8 GeV e- synchroton
1 GeV e- Linac
NewSUBARU
MeV γ

NewSUBARU (Japan)

0.55 – 1.5 GeV storage ring

E_γ=0.5 – 76 MeV
I_γ = 10^6 – 10^7 s^{-1}
(3 – 6 mm dia.)
$\Delta E/E$ > 2%

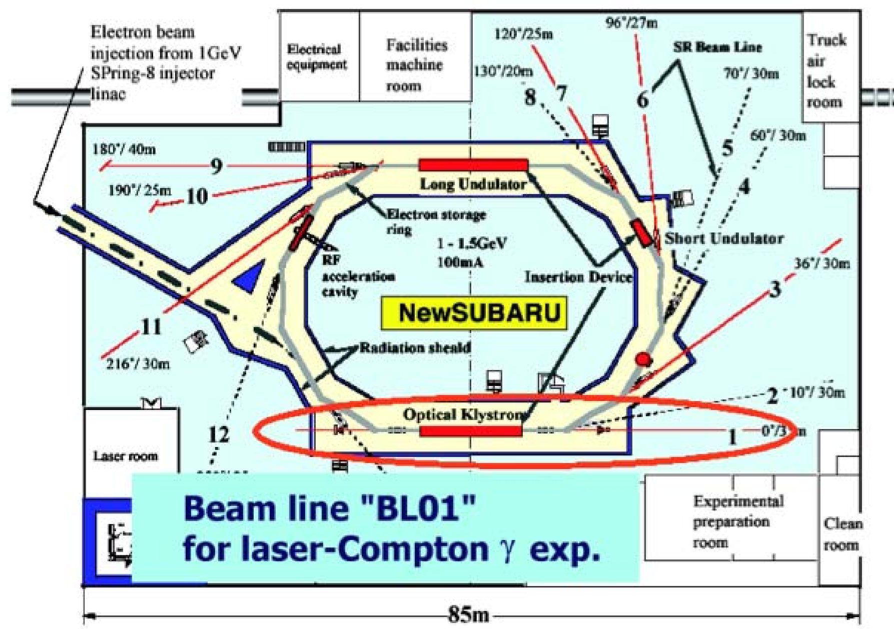

Experimental Hutch GACKO (Gamma Collaboration Hutch of Konan University)

Table-top Lasers

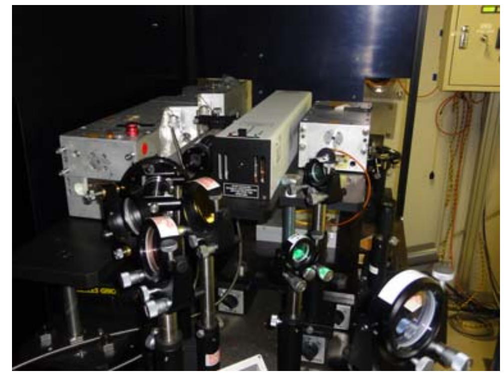

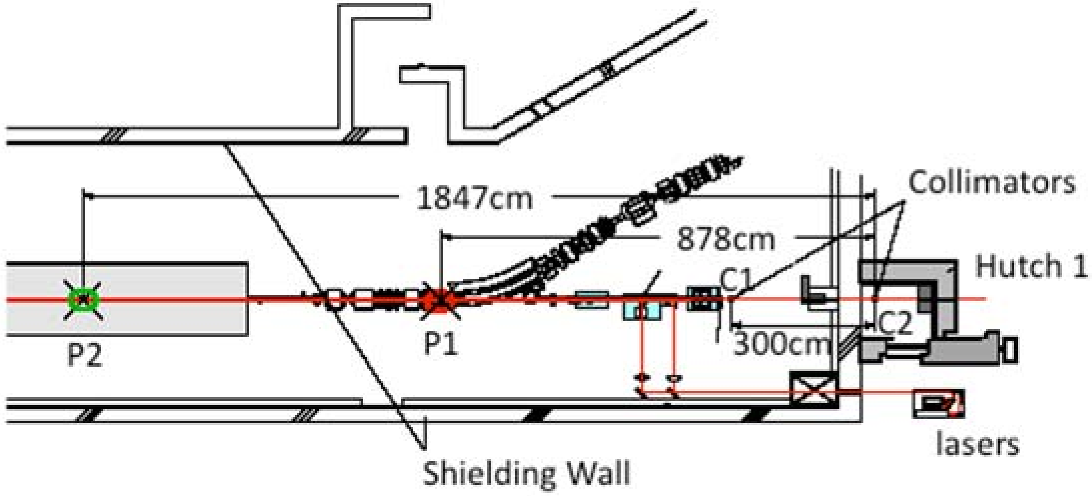
1847cm
878cm
Collimators
Hutch 1
C1
C2
300cm
P2
P1
lasers
Shielding Wall

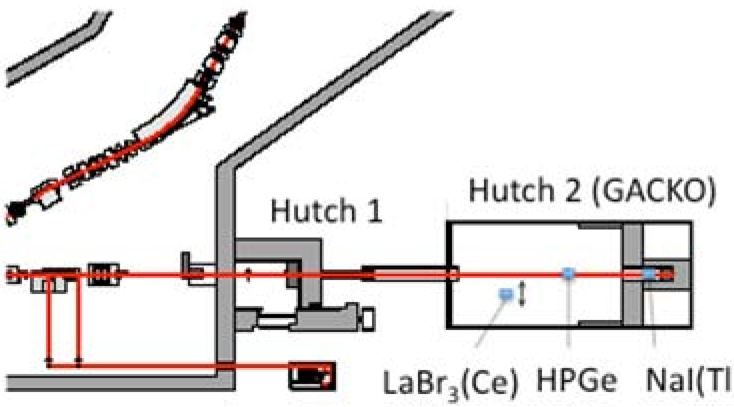
Hutch 1
Hutch 2 (GACKO)
LaBr3(Ce)
HPGe
NaI(Tl)

LCS γ-ray beams and response functions of a 3.5" x 4.0" $LaBr_3(Ce)$ detector

Double collimation C1: 6mm, C2: 2mm

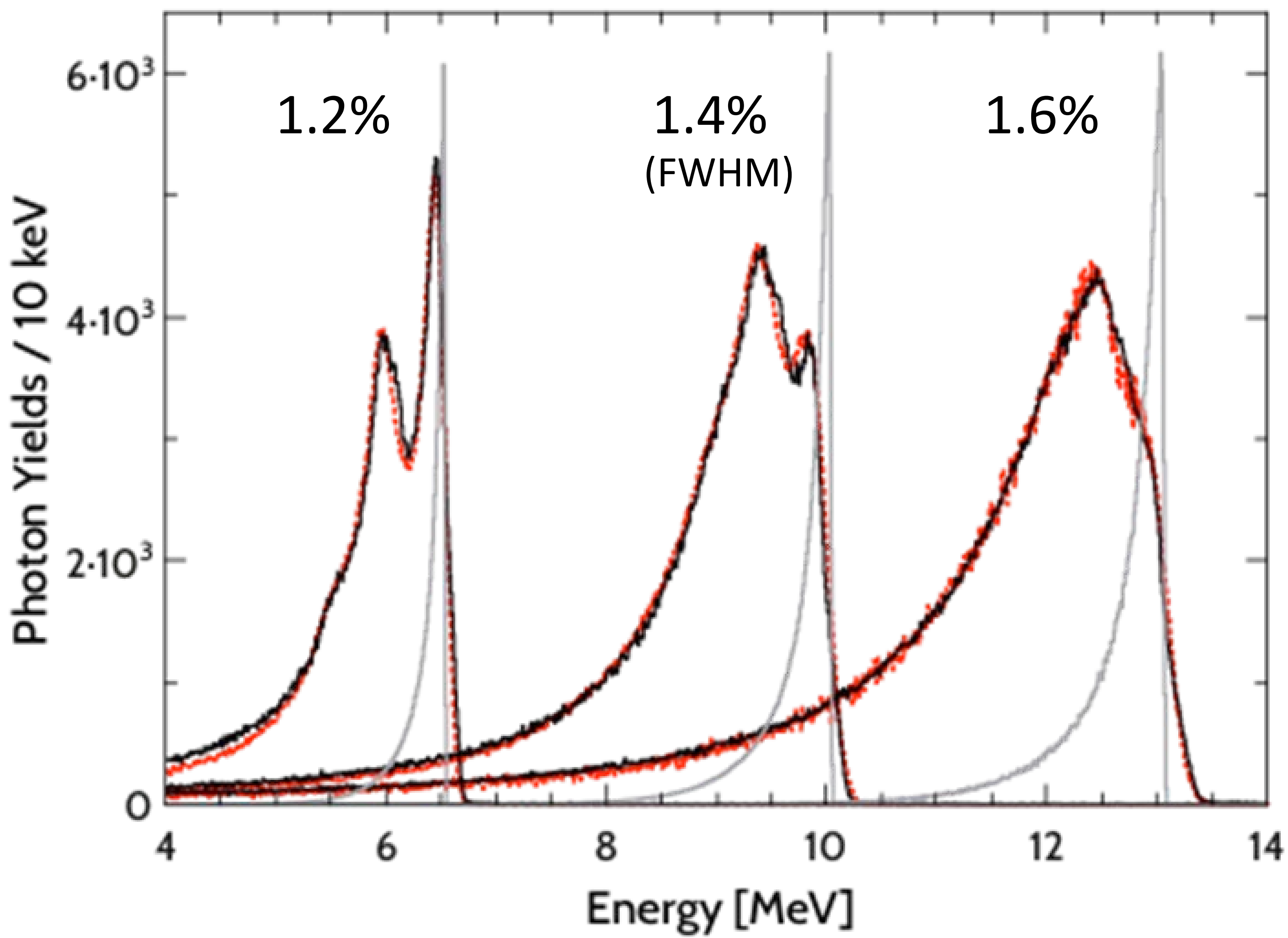

γ-ray strength function

6 MeV for odd-N nuclei ⟵ $S_{n:}$ ⟶ 12 MeV for even-even nuclei

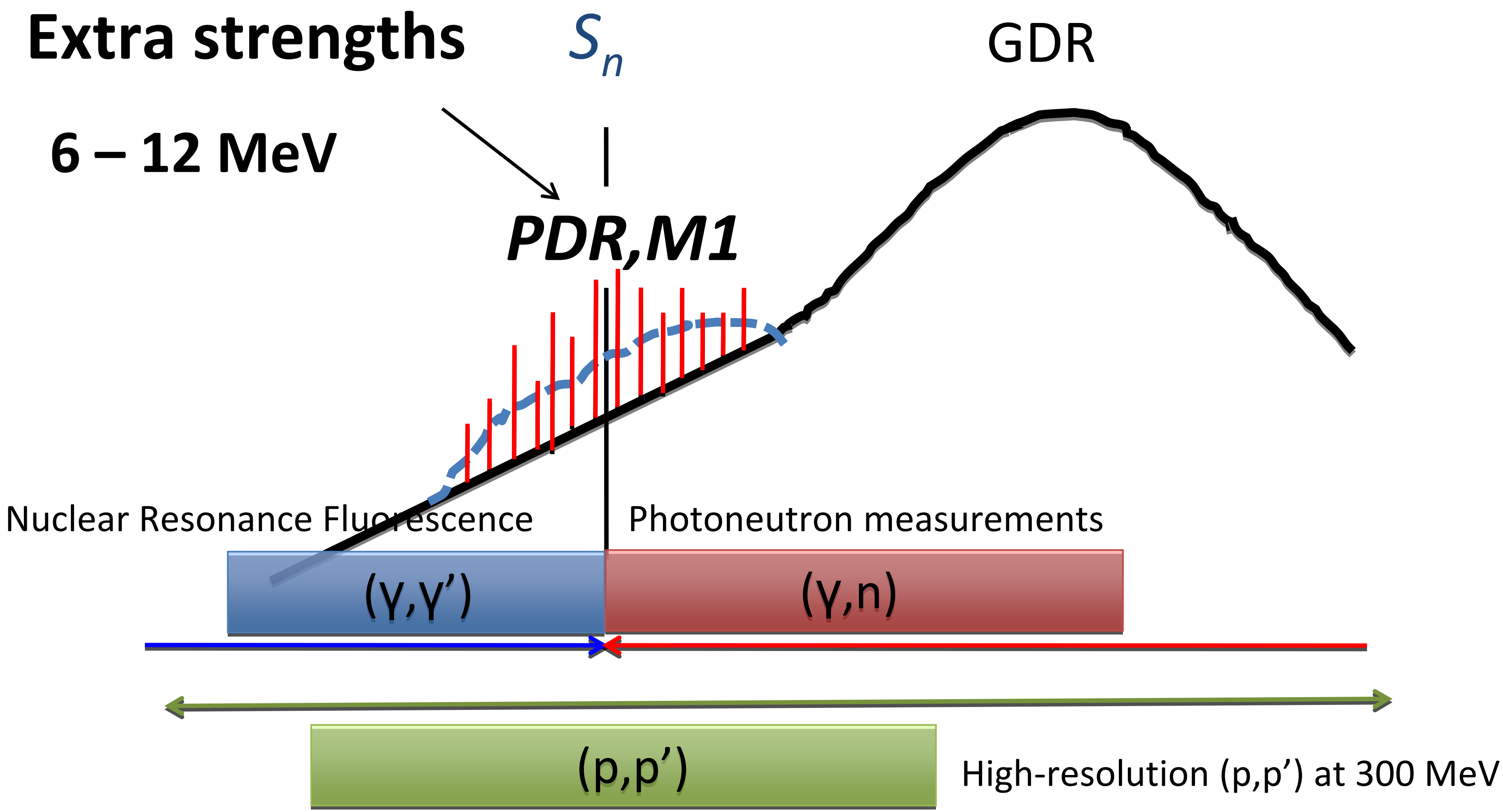

Courtesy by A. Tonchev

Spin and Parity Determination

^{138}Ba

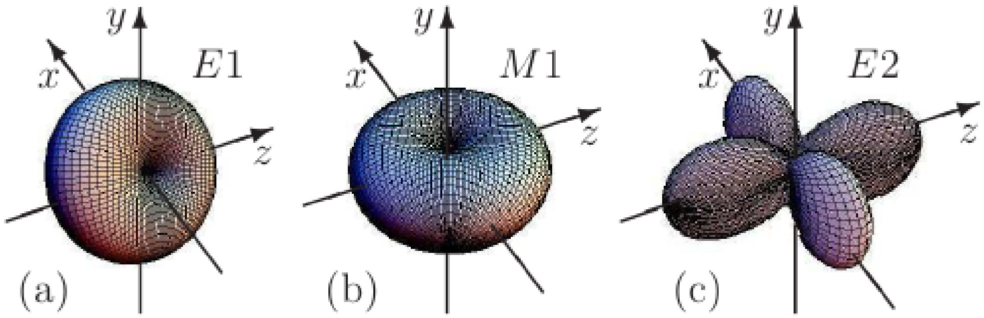

z axis: beam direction; x axis: vector of polarization

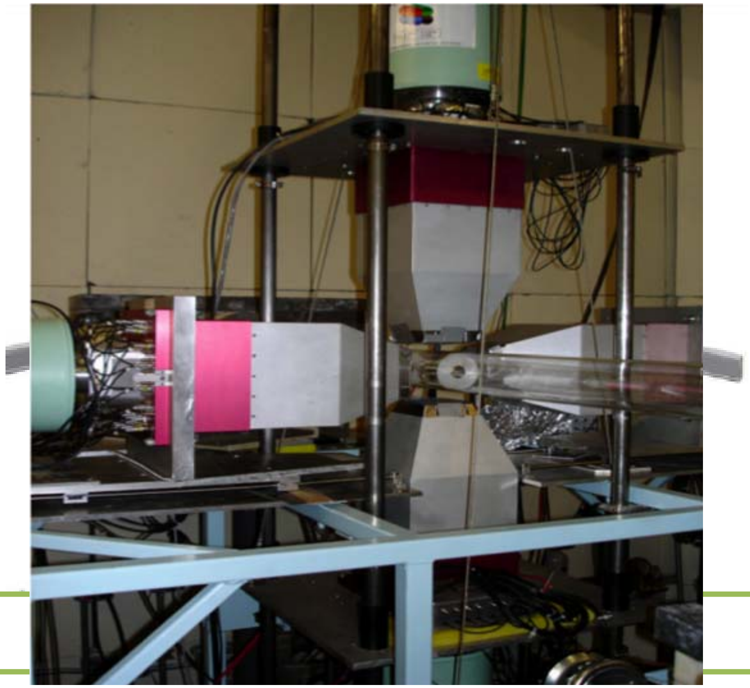

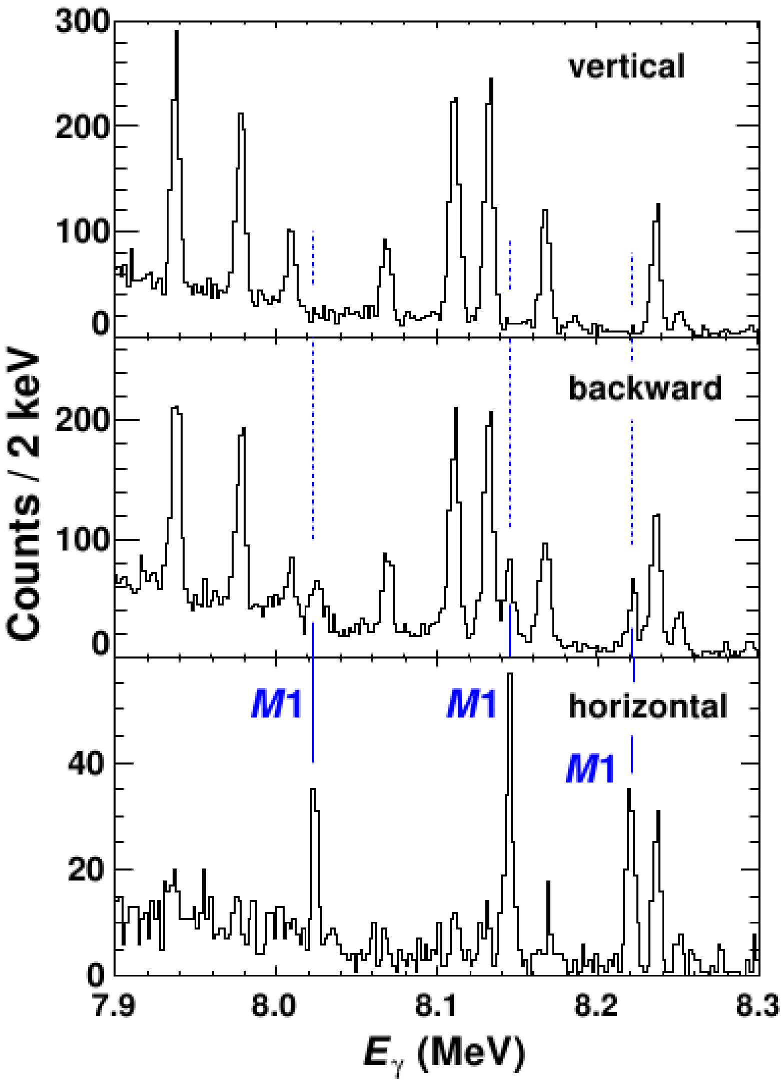

N. Pietralla, at al. PRL **88** (2002) 012502; A. Tonchev, NIM **B 241** (2005) 51474

Resonances above S_n

Threshold Photoneutron Technique
Bremsstrahlung + n-TOF

C.D. Berman et al., PRL25, 1302 (1970)
R.J. Baglan et al., PRC3, 2475 (1971)

$^{207}Pb(\gamma,n)$

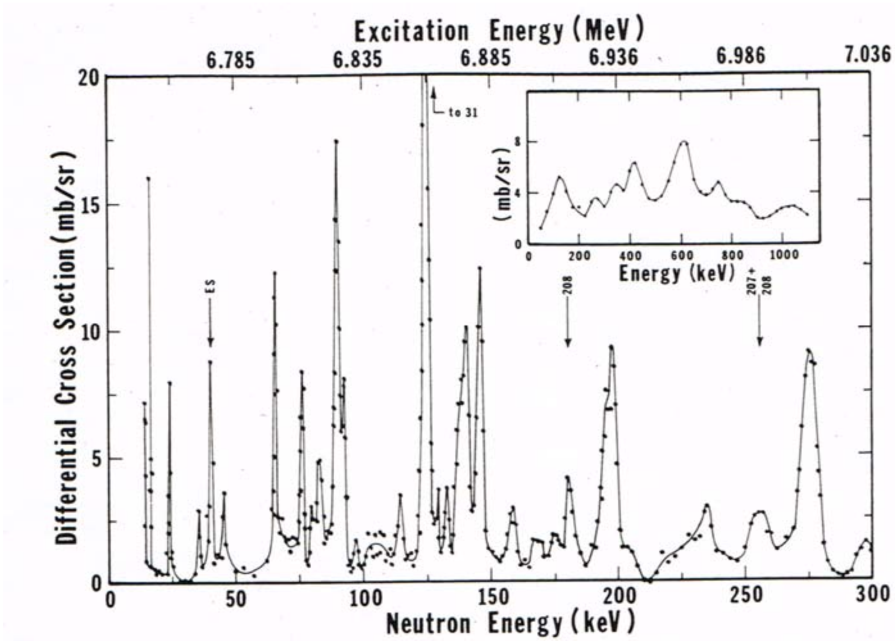

$^{208}Pb(\gamma,n)$

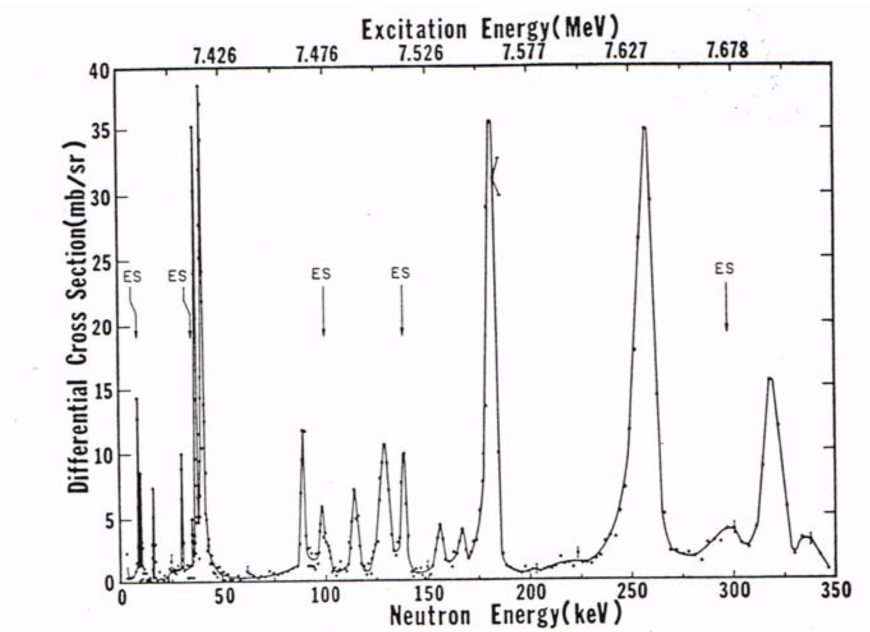

(p,p') near 0^{o} as Coulomb excitation of PDR

C. Iwamoto *et al.*, Phys. Rev. Lett. 108, 262501 (2012)

^{90}Zr(p,p') at 295 MeV

Multipole-decomposition analysis of the proton angular distribution

PDR in Lorentzian shape

B(E1)↑□0.75 ± 0.08 e^{2} fm^{2} E=7-11 MeV
TRK sum rule 2.1±0.2%

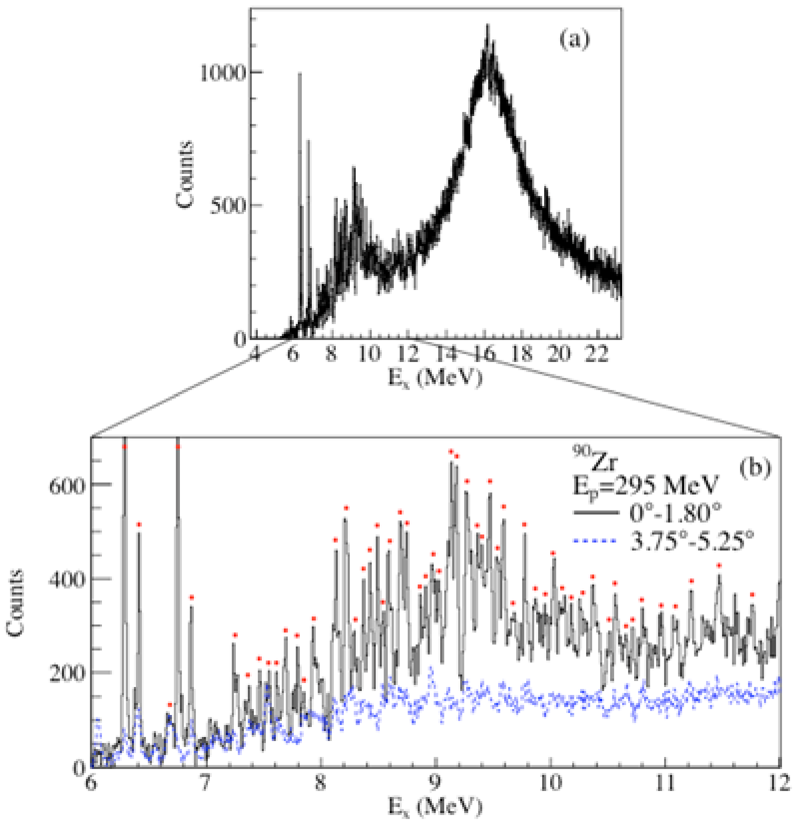

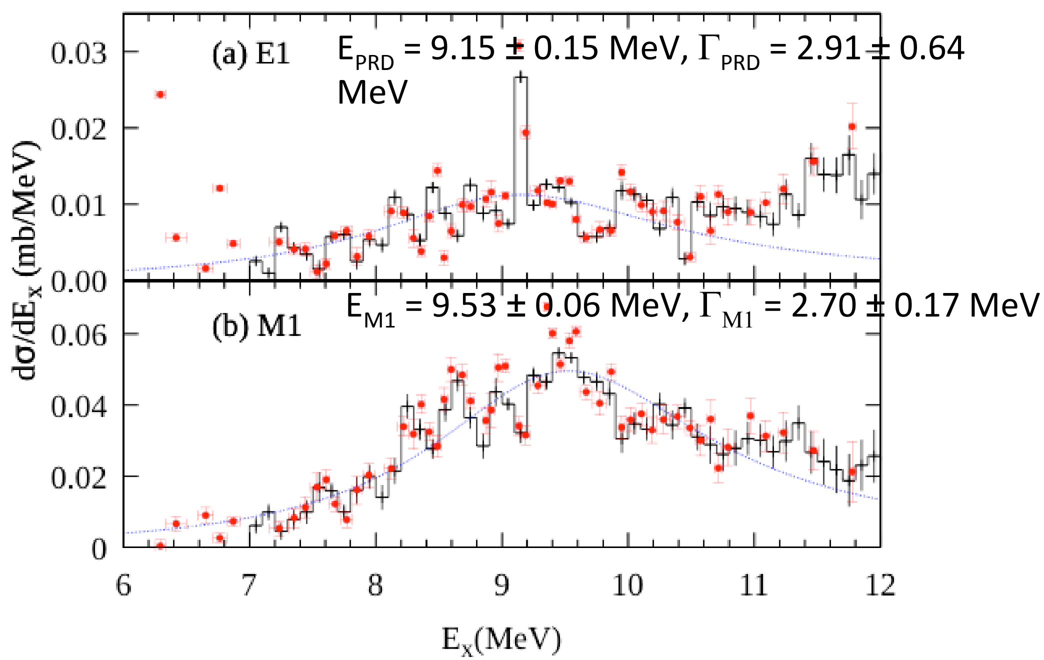

E1 and M1 photoexcitations in ^{208}Pb

$$\ell = 0$$

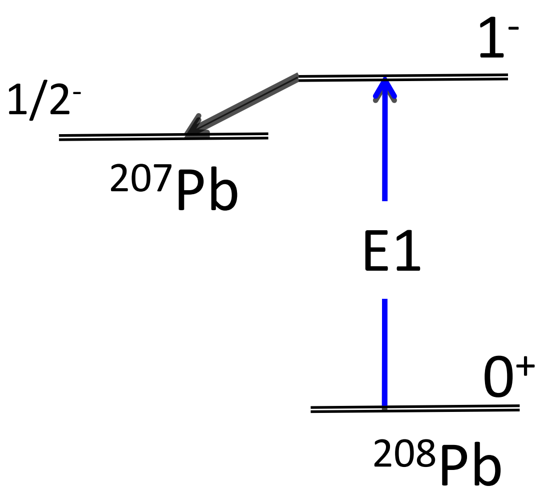

$$\ell = 1$$

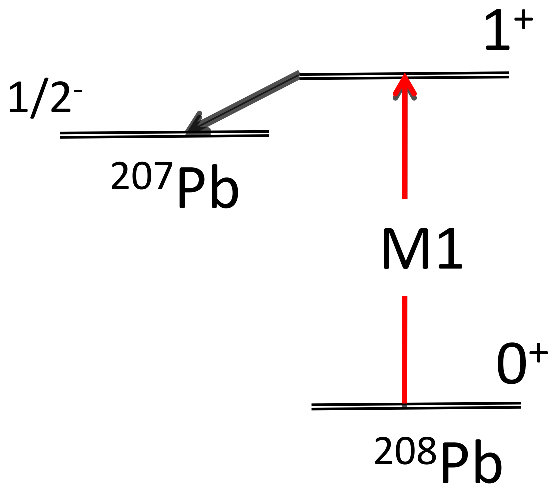

E1 and M1 photoexcitations in ^{207}Pb

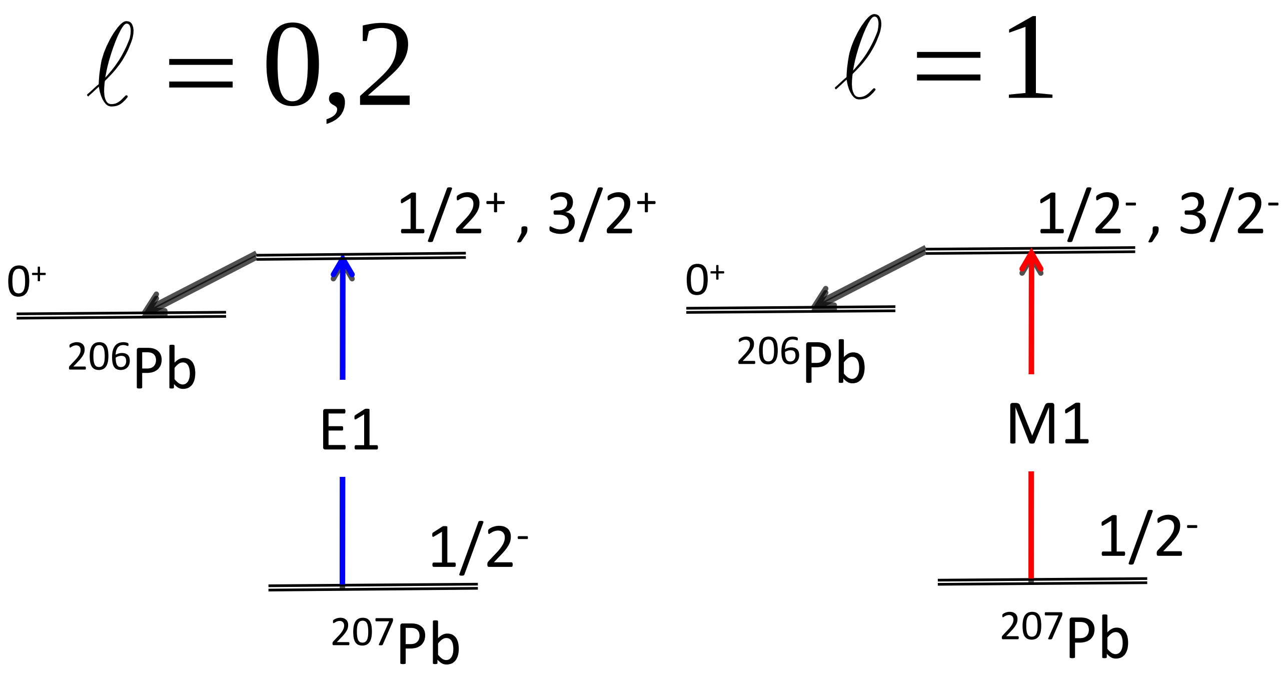

PDR in ^{207,208}Pb

T. Kondo *et al.*, Phy. Rev. C 86, 014316 (2012)

Linear polarization
P=93.4±0.7%

Targets
9587 mg, 98.5%, 208Pb
3482 mg, 99.1%, 207Pb

Neutron Detector
High- and flat-efficiency long counters
East & Walton, NIM 72 (1969)

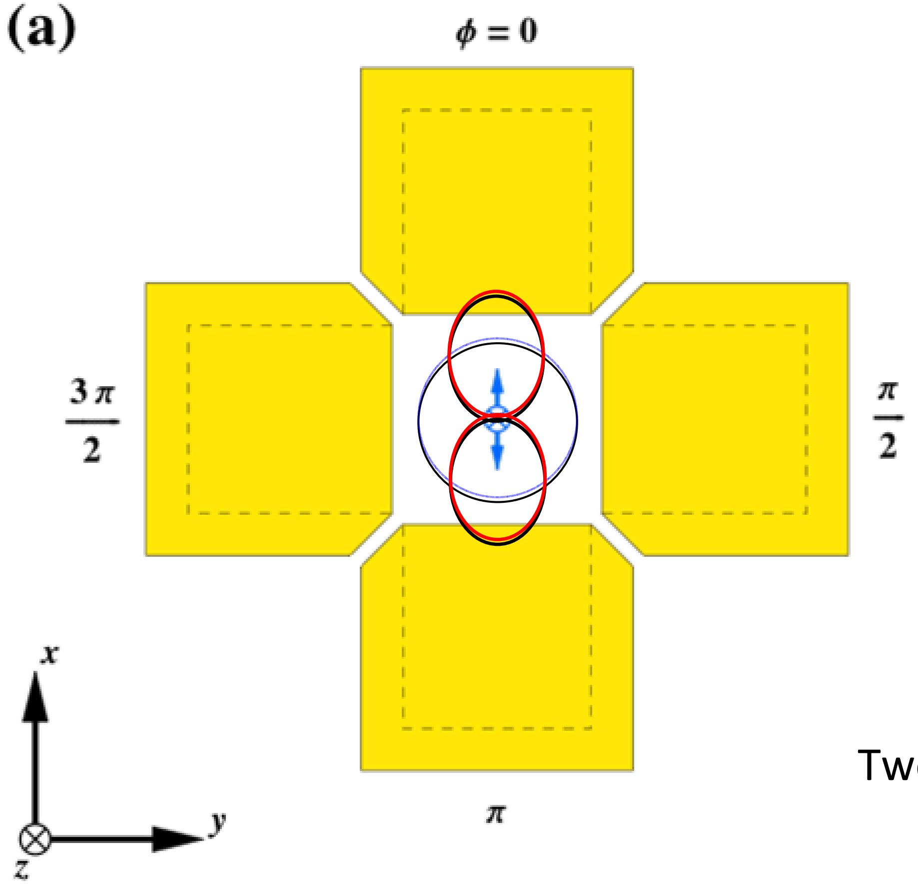

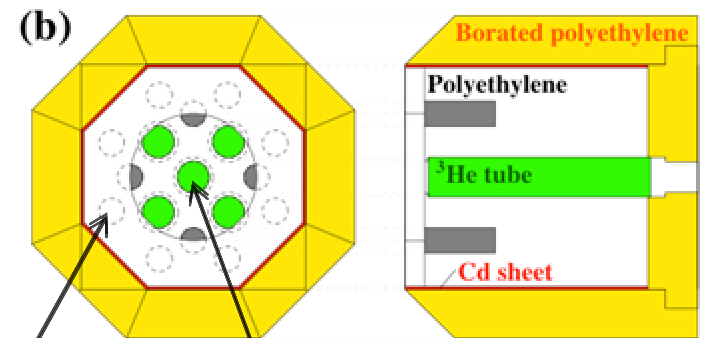

Five 3He proportional counters

Twelve neutron-guiding holes

Angular distributions and Detection efficiencies of neutrons

s-wave neutrons

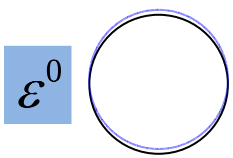

$$W^{s}(\theta,\phi) = \frac{1}{4\pi}$$

p-wave neutrons

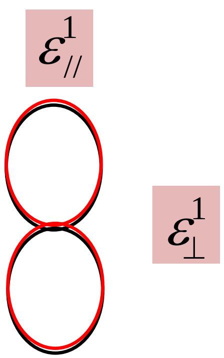

$$W^{p}_{pol}(\theta,\phi) = \frac{3}{8\pi}[\sin^2\theta(1+\cos 2\phi)]$$

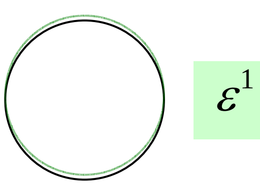

$$W^{p}_{unpol}(\theta,\phi) = \frac{3}{8\pi}\sin^2\theta$$

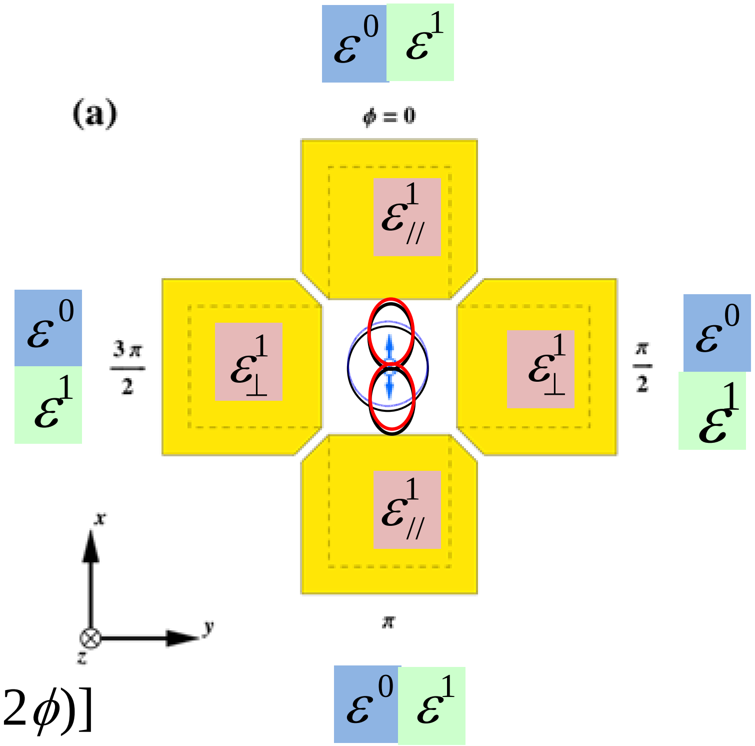

Circularly-polarized photons

Detection efficiencies

ε^0 252Cf source

$\varepsilon^1_{//}$

$\varepsilon^1_{\perp}$

ε^1

MCNP Monte Carlo simulations

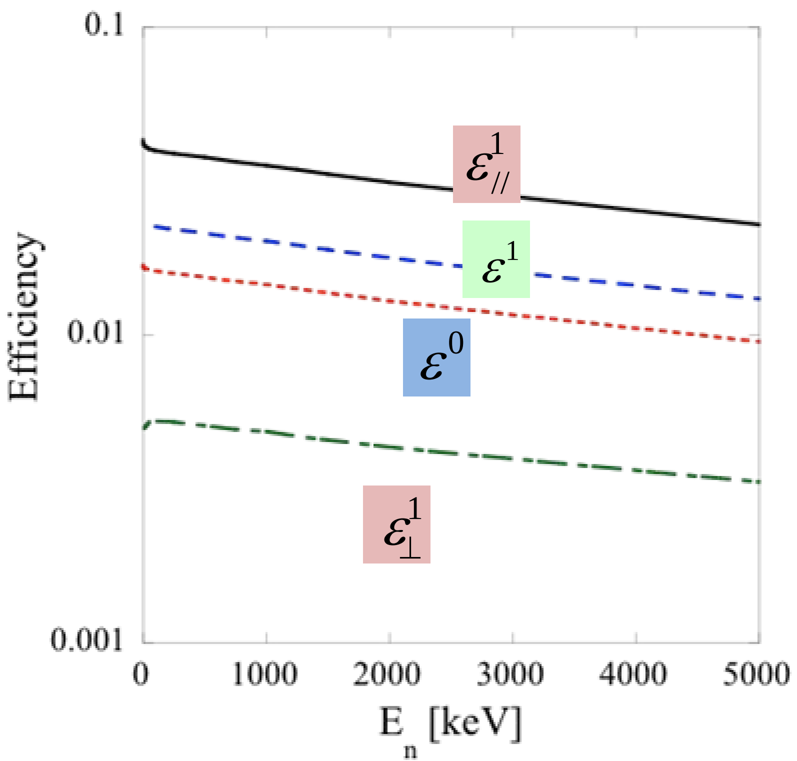

PDR in ^{207,208}Pb above neutron threshold

T. Kondo *et al*., Phy. Rev. C 86, 014316 (2012)

9587 mg, 98.5%, 208Pb
3482 mg, 99.1%, 207Pb

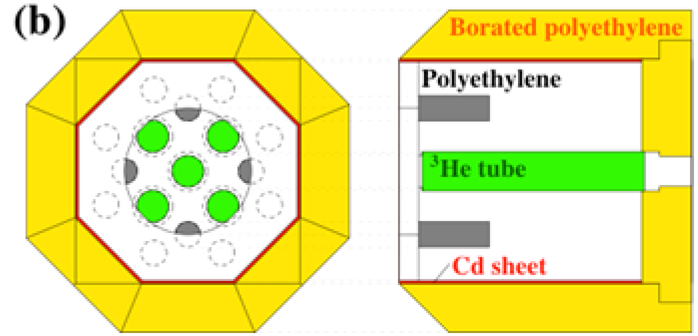

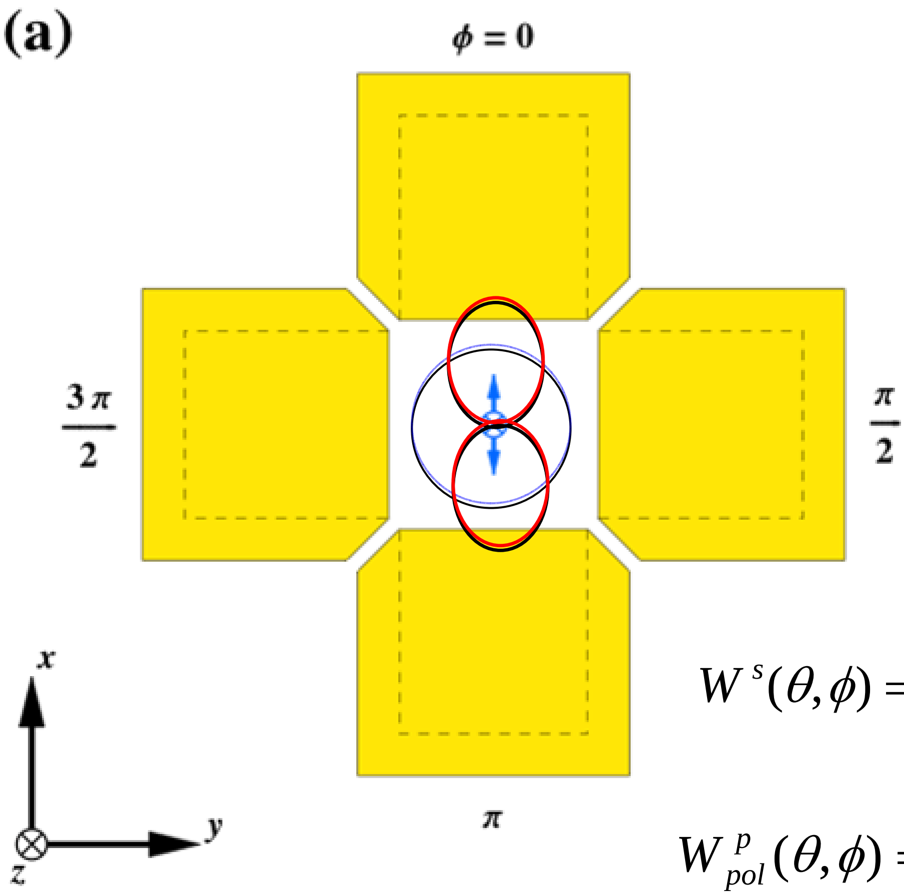

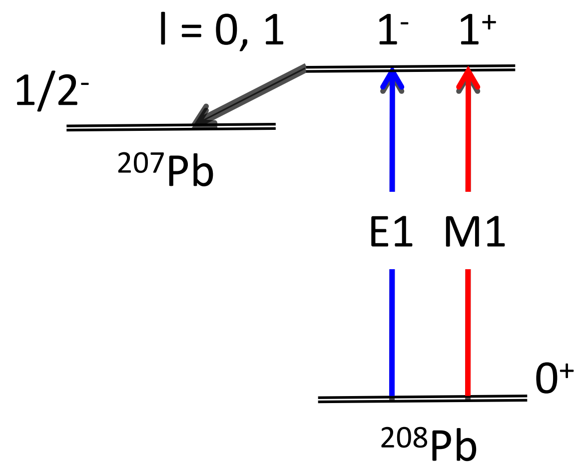

$$W^{s}(\theta,\phi) = \frac{1}{4\pi}$$

$$W^{p}_{pol}(\theta,\phi) = \frac{3}{8\pi}[\sin^2\theta(1+\cos 2\phi)]$$

Neutron anisotropy detector for E1 & M1 (γ,n) cross section measurements

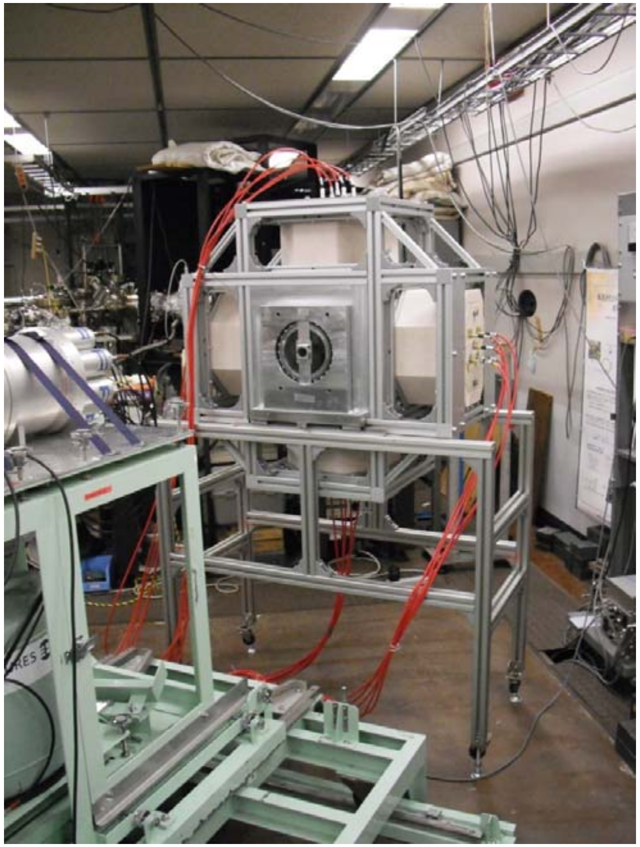

E1 cross sections for ^{208,207}Pb

<u>HFB+QRPA E1 strength</u> plus
pygmy E1 resonance
in Lorentzian shape

E_o = 7.5 MeV, Γ = 0.4 MeV
$\sigma_o \approx$ 20 mb for 208Pb
$\sigma_o \approx$ 15 mb for 207Pb

TRK sum rule
0.42% for 208Pb
0.32% for 207Pb

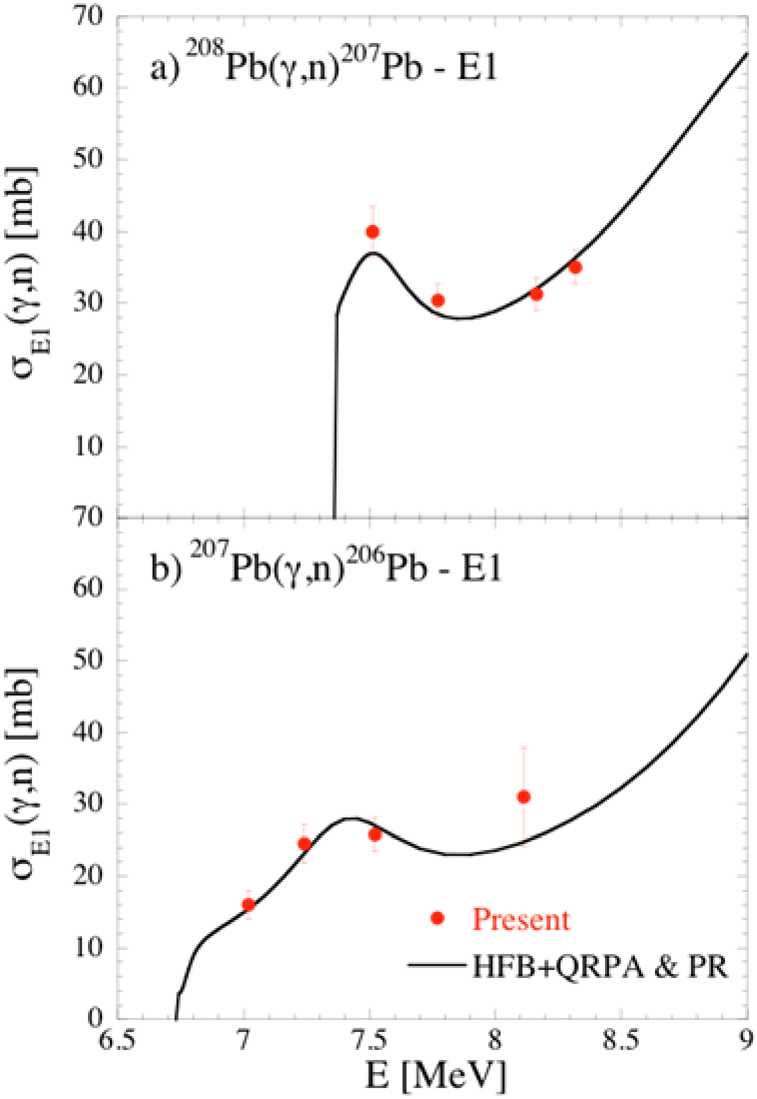

$$B(E1)\uparrow$$

208Pb

Present

$$B(E1)\uparrow = 0.82 \pm 0.09\ e^2 \cdot fm^2$$
$$E = 7.51 - 8.32\ MeV$$

(p,p') experiment

$$B(E1)\uparrow = 0.982 \pm 0.206\ e^2 \cdot fm^2$$
$$E = 7.515 - 8.430\ MeV$$

207Pb

$$B(E1)\uparrow = 0.88 \pm 0.17\ e^2 \cdot fm^2$$
$$E = 7.02 - 8.32\ MeV$$

Comparisons

E1

Present results

B(E1)⇧=0.82±0.09 e^2 fm^2 for 208Pb E=7.51 – 8.32 MeV

B(E1)⇧=0.88±0.17 e^2 fm^2 for 207Pb E=7.02 – 8.11 MeV

(p,p') I. Poltoratska et al., PRC 85, 041304(R) (2012)

B(E1)⇧=0.982±0.206 e^2 fm^2 for 208Pb E=7.515 – 8.430 MeV

M1 cross sections for ^{208,207}Pb

208Pb

B(M1)=4.2 ± 2.3 μ_N^2 E=7.51-8.32 MeV

E_o = 8.06 MeV, Γ= 0.6 MeV
σ_o = 3.6 mb

207Pb

B(M1)=4.0 ± 1.9 μ_N^2 E=7.02-7.52 MeV

$E_o \approx$ 7.25 MeV, $\Gamma \approx$ 1 MeV
$\sigma_o \approx$ 3.2 mb

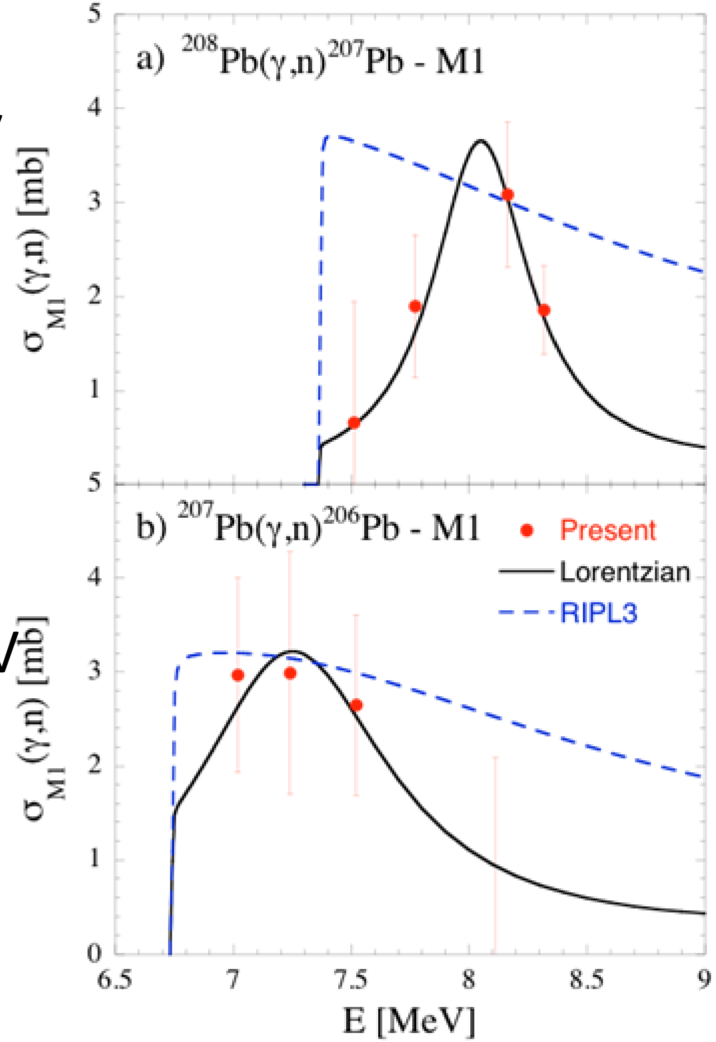

M1 strength
in Lorentzian shape

Comparisons

M1

Present results

B(M1)⇧=4.2±2.3 μ_N^2 for 208Pb E=7.51 – 8.32 MeV

B(M1)⇧=4.0±1.9 μ_N^2 for 207Pb E=7.02 – 7.52 MeV

207Pb+n R. Köhler et al., PRC 35, 1646 (1987)

B(M1)⇧=5.8 μ_N^2 for 208Pb E=7.37 – 8.0 MeV

Please formulate angular distributions for d- and f-wave neutrons.

$W(\theta, \phi)$

$$\vec{\gamma} + {}^{A}X \rightarrow {}^{A}X^{*} \rightarrow {}^{A-1}X + n$$ (d, f waves)

s-wave $$W^{s}(\theta, \phi) = \frac{1}{4\pi}$$

p-wave $$W^{p}_{pol}(\theta, \phi) = \frac{3}{8\pi}[\sin^{2}\theta(1+\cos 2\phi)]$$

Nucleosynthesis of light nuclei

Reciprocity Theorem

A + a ⟶ B + b + Q

B + b ⟶ A + a – Q   Q value

$$\frac{\sigma(b \to a)}{(2I_A+1)(2i_a+1)p_a^2} = \frac{\sigma(a \to b)}{(2I_B+1)(2i_b+1)p_b^2}$$

Neutron Channel

a=n, b=γ $p_\gamma = \hbar k = \frac{E_\gamma}{c}$ $p_n^2 = 2\mu E_n$ $2j_b + 1 \to 2$

Equivalency between (n, γ) and (γ,n)

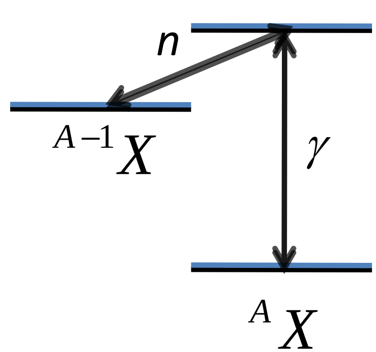

Examples

D

Big Bang Nucleosynthesis: p(n,γ)D vs D(γ,n)p

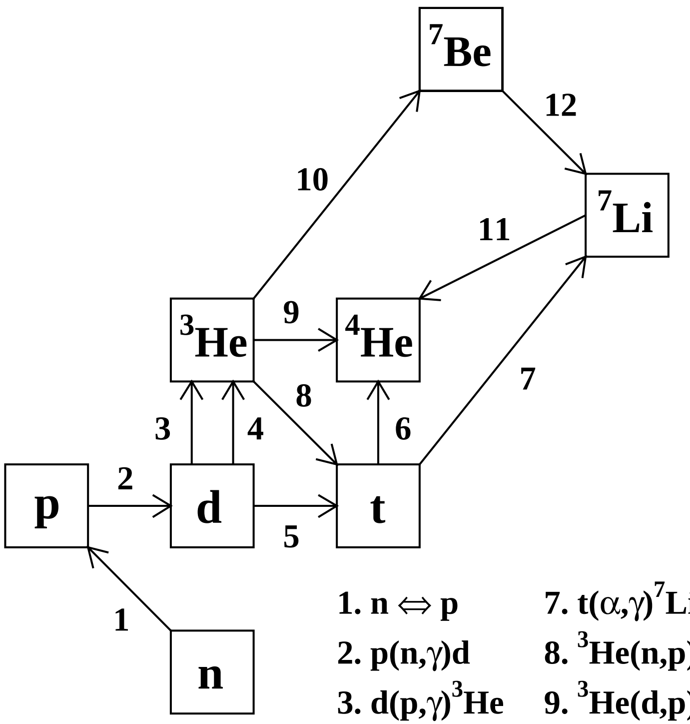

1. n $\Leftrightarrow$ p
2. p(n,γ)d
3. d(p,γ)^{3}He
4. d(d,n)^{3}He
5. d(d,p)t
6. t(d,n)^{4}He
7. t(α,γ)^{7}Li
8. ^{3}He(n,p)t
9. ^{3}He(d,p)^{4}He
10. ^{3}He(α,γ)^{7}Be
11. ^{7}Li(p,α)^{4}He
12. ^{7}Be(n,p)^{7}Li

Examples

D Big Bang Nucleosynthesis: p(n,γ)D vs D(γ,n)p

K.Y. Hara et al., PRD 68, 072001 (2003)

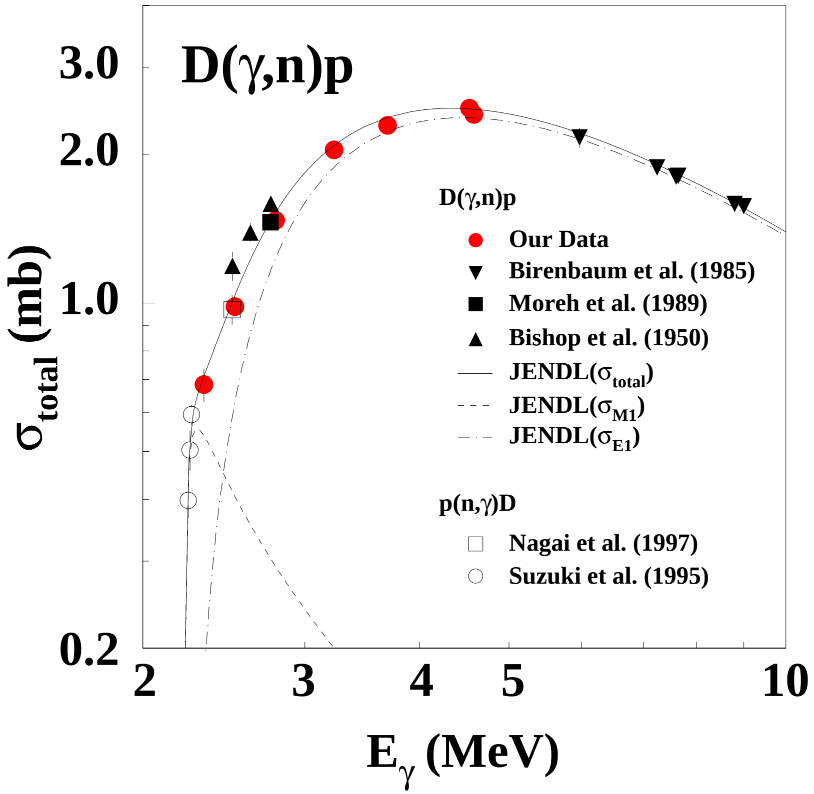

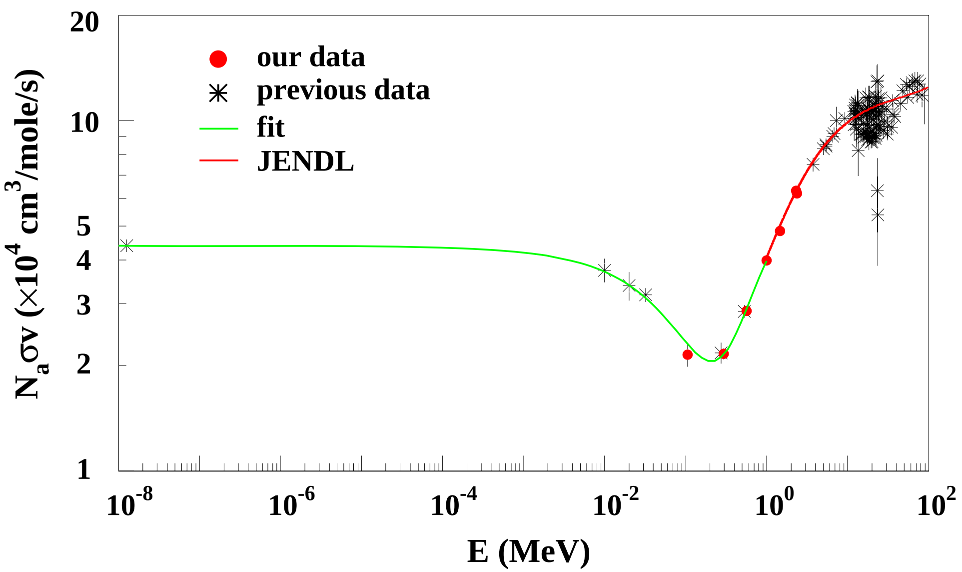

Examples

9Be Supernova Nucleosynthesis

$$\alpha\ \alpha \rightleftarrows {}^{8}Be(n,\gamma)\,{}^{9}Be \quad vs \quad {}^{9}Be(\gamma,n){}^{8}Be$$

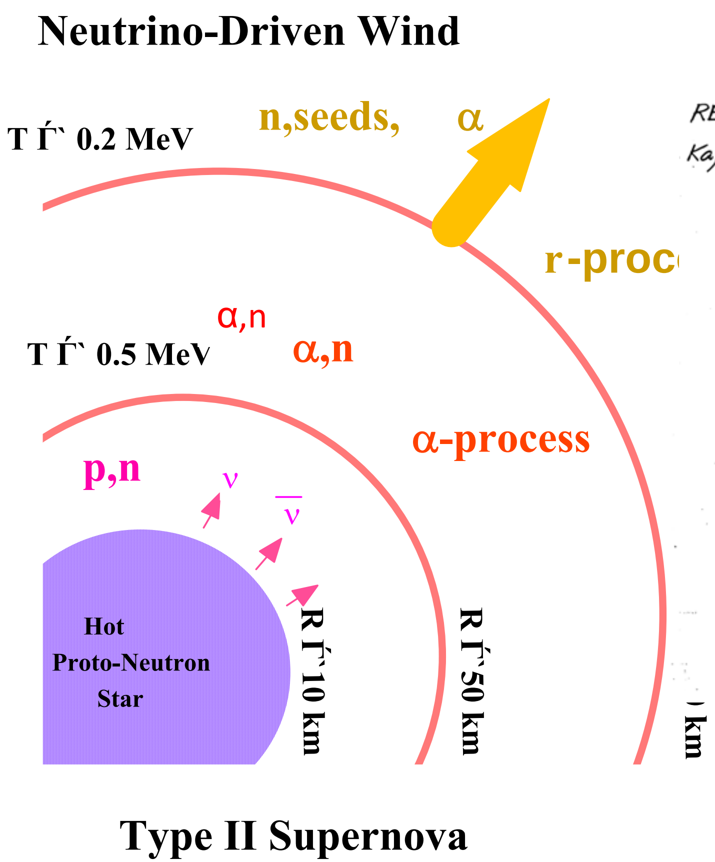

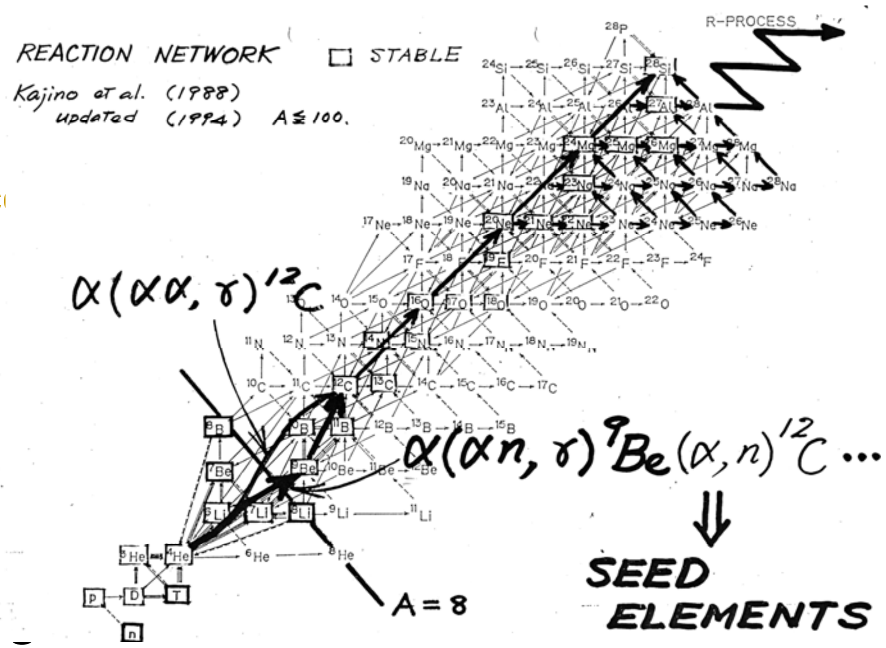

Examples

9Be   Supernova Nucleosynthesis

$\alpha\ \alpha \rightleftarrows {}^{8}Be(n,\gamma)\, {}^{9}Be$ vs ${}^{9}Be(\gamma,n){}^{8}Be$

H. Utsunomiya *et al.* PRC 63, 018801 (2001)
K. Sumiyoshi *et al*. NPA709, 467 (2002)

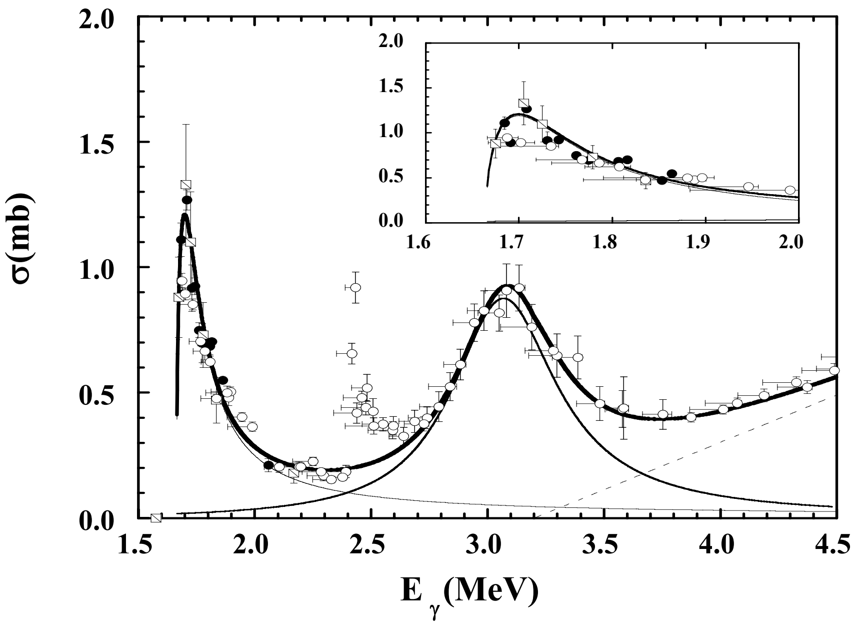

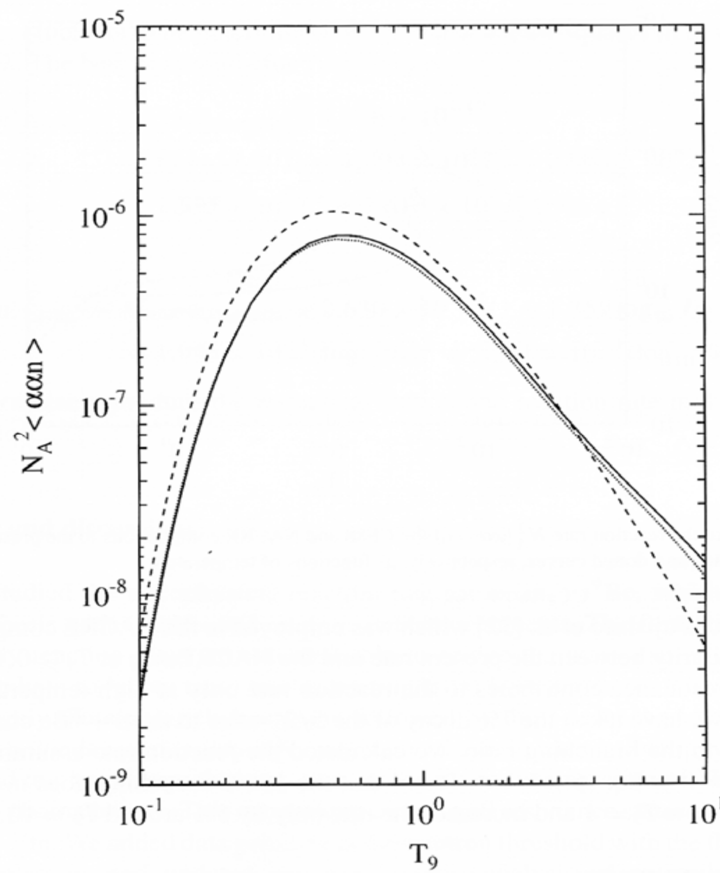

Examples

9Be

Supernova Nucleosynthesis

$\alpha\,\alpha \rightleftarrows {}^{8}Be(n,\gamma)\,{}^{9}Be$ vs ${}^{9}Be(\gamma,n){}^{8}Be$

C.W. Arnold *et al*. PRC 85, 044605 (2012)

HIGS

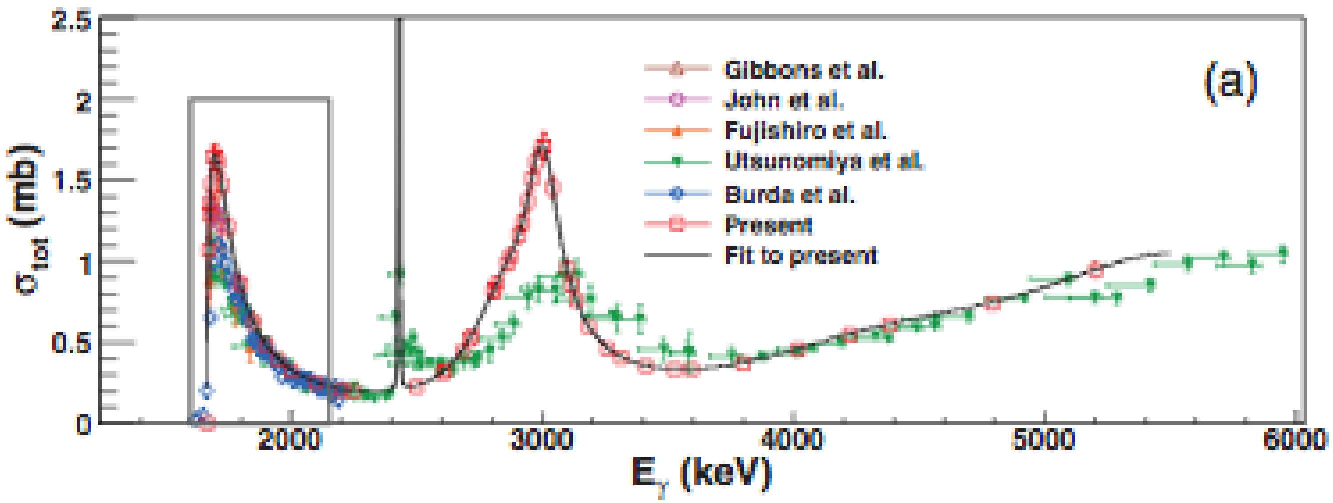

A new measurement has been done by Konan University and CNS, University of Tokyo etc. at the NewSUBARU synchrotron radiation facility and data reduction is in progress.

p-nuclei

35 neutron-deficient nuclei from Se(Z=34) to Hg(Z=80)

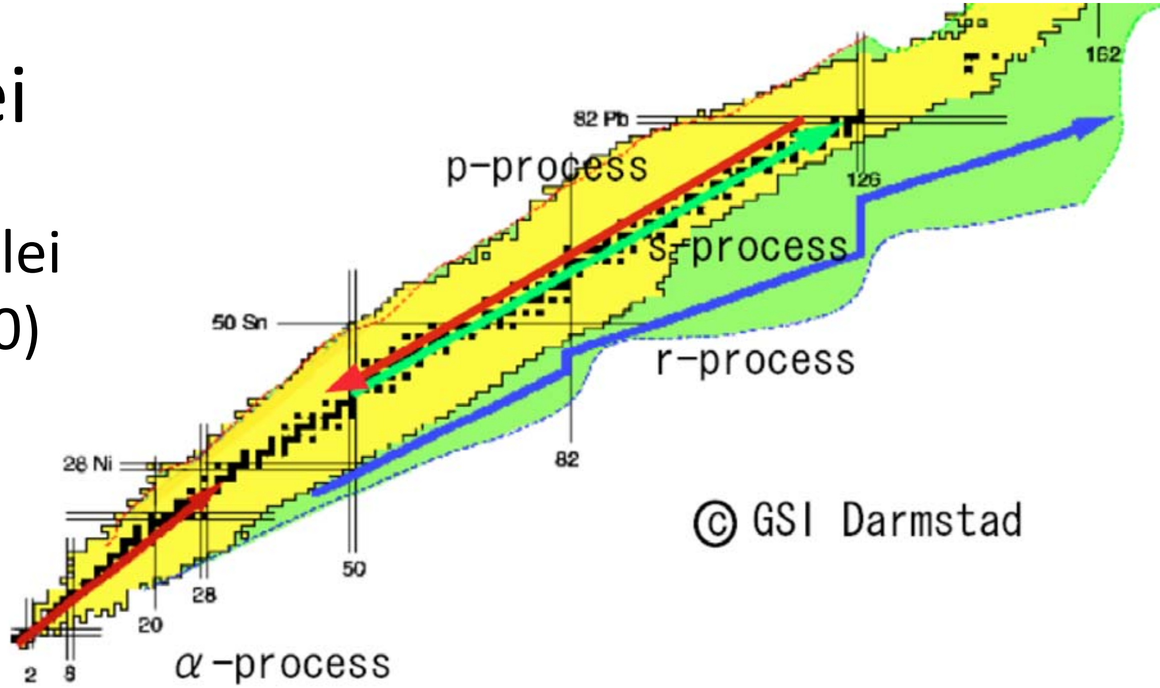

$(p,\gamma)+\beta-decay$

$(\gamma,n)+(\gamma,p)$

$(\gamma,n)+(\gamma,\alpha)+\beta-decay$

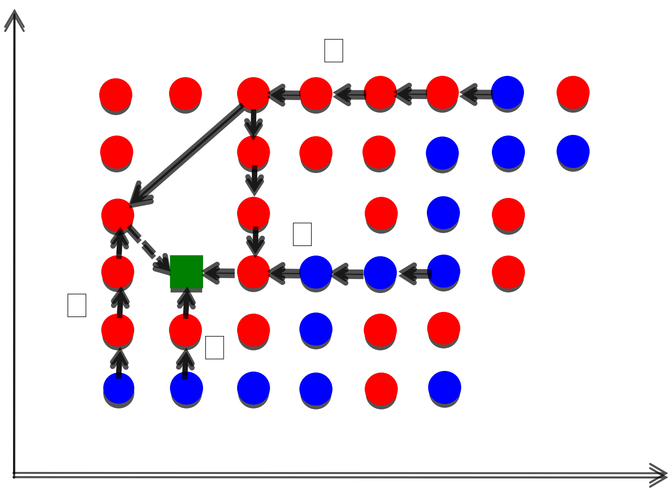

(p,γ)

(γ,n)

Nucleosynthesis of Heavy Elements
s-process, r-process and p-process

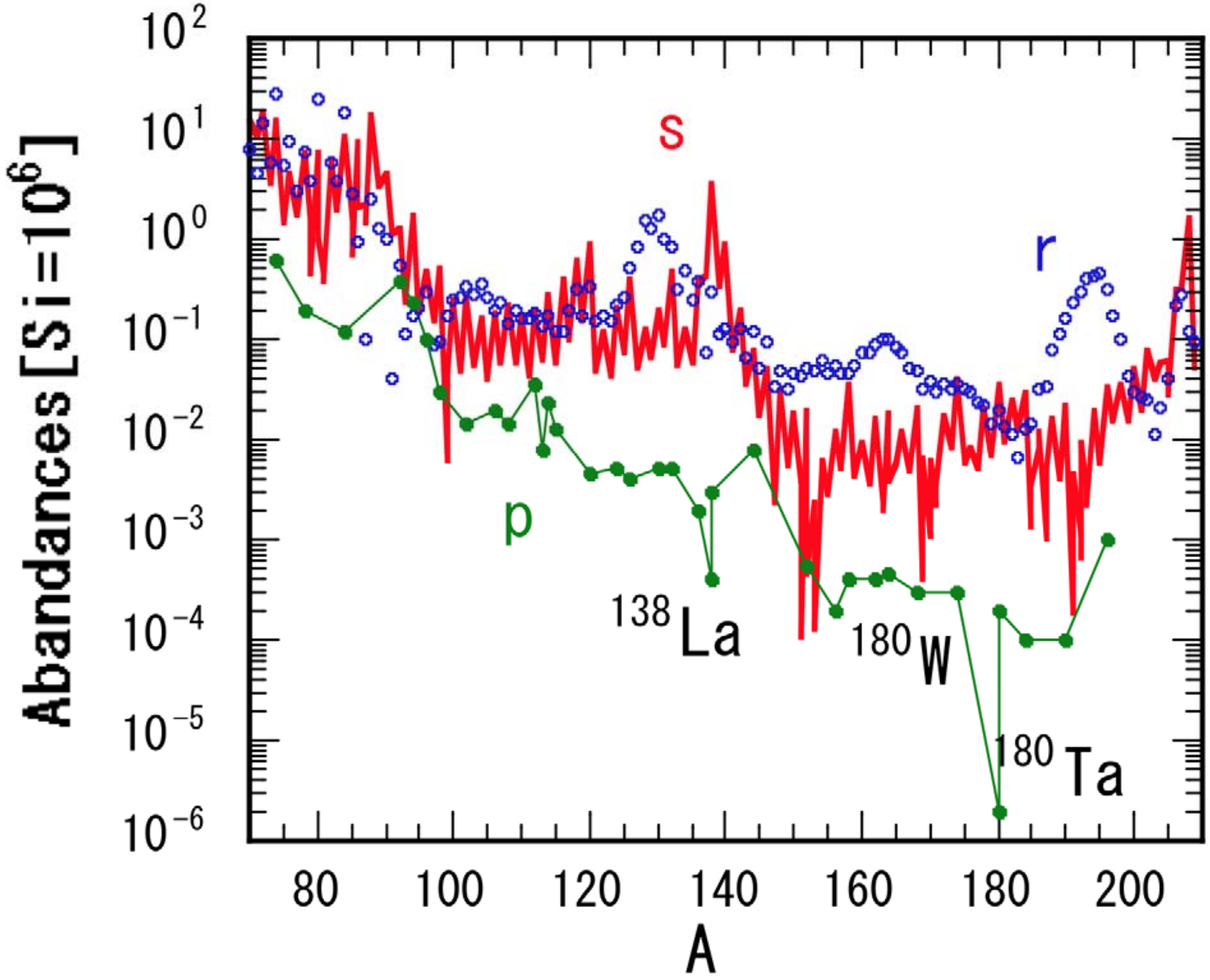

p-process nucleosynthesis

P. Mohr et al., Phys. Lett. B 488 (2000) 127
H. Utsunomiya et al., Nucl. Phys. A 777 (2006) 459

Photoreaction rates for gs

$$\lambda_{\gamma n}(T) = \int_0^\infty c n_\gamma(E,T)\sigma_{\gamma n}(E)dE$$

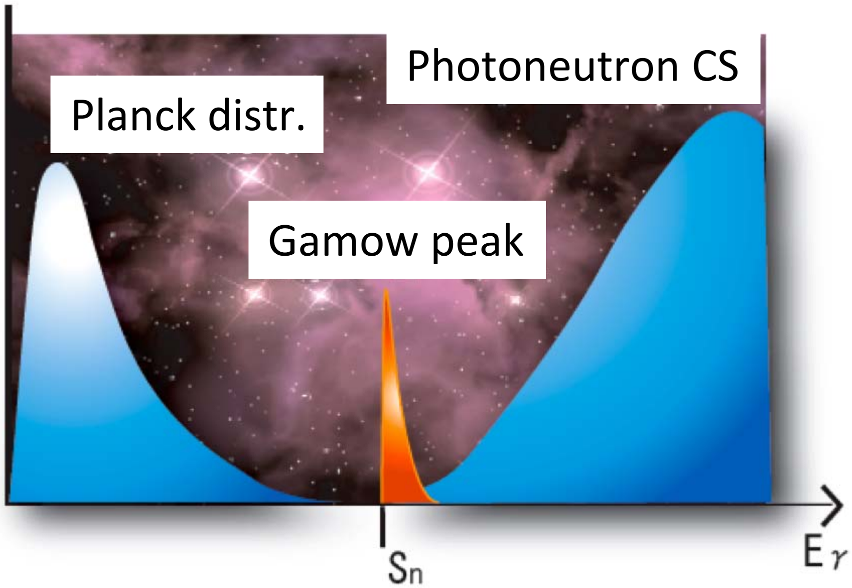

Planck distribution

$$n_\gamma(E,T)dE = \frac{1}{\pi^2}\frac{1}{(\hbar c)^3}\frac{E^2}{\exp(E/kT)-1}dE$$

Stellar photoreaction rate

Photoreaction rates for a state μ

$$\lambda_{\gamma n}^{\mu}(T) = \int_0^{\infty} c n_\gamma(E,T)\sigma_{\gamma n}^{\mu}(E)dE$$

Stellar photoreaction rate

$$\lambda_{\gamma n}^{*} = \frac{\sum_\mu (2j^\mu+1)\lambda_{\gamma n}^{\mu}(T)\exp(-\varepsilon_\mu/kT)}{\sum_\mu (2j^\mu+1)\exp(-\varepsilon_\mu/kT)}$$

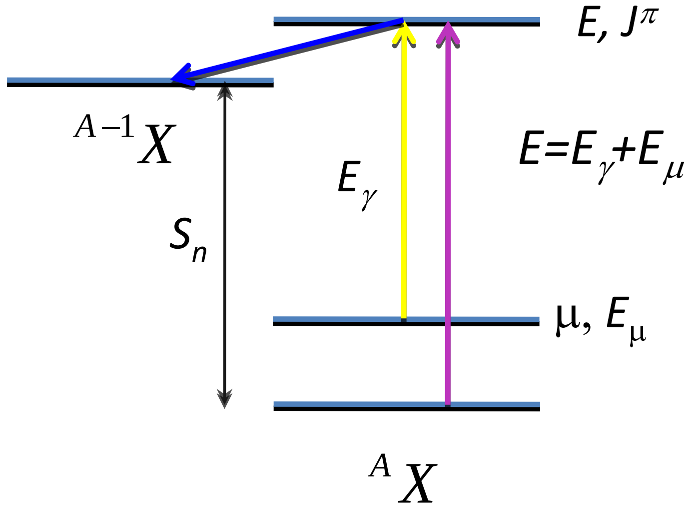

$$\sigma_{\gamma n}^{\mu}(E_\gamma) = \pi D_\gamma^2 \frac{1}{2(2j^\mu+1)}\sum_{J^\pi}(2J+1)\frac{T_\gamma^\mu(E_\gamma,J^\pi)T_n(E,J^\pi)}{T_{tot}(E,J^\pi)}$$

$$T_\gamma^\mu(E_\gamma,J^\pi) = 2\pi\varepsilon_\gamma^3 f_\gamma(E_\gamma)\uparrow$$ for E1 transition

Key quantity:

γ-ray strength function $f_\gamma(E_\gamma)$

$E_\gamma > S_n$ for gs

$E_\gamma < S_n$ for excited states μ

Only naturally occurring isomer $^{180}Ta^{m}$

- Odd-odd Nucleus (Z=73, N=107)
- Neutron deficient nucleus (classified as one of p-nuclei)
- Solar Abundance ; 2.48×10^{-6}(the rarest)
- Half Life > 1.2×10^{15}y
- E_x = 75keV
- $J^{\pi} = 9^{-}$

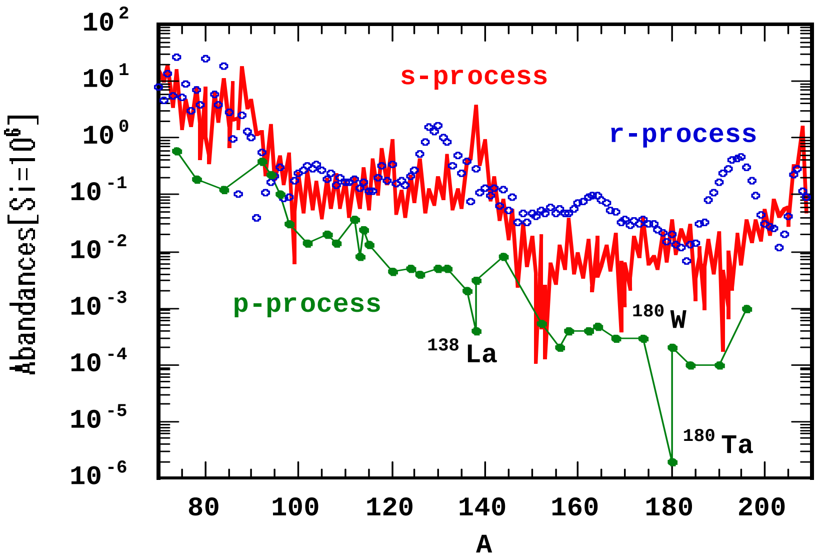

$^{180}Ta^{gs}$

•Half Life = 8.152h

•$J^{\pi} = 1^{+}$

Network of nucleosynthesis

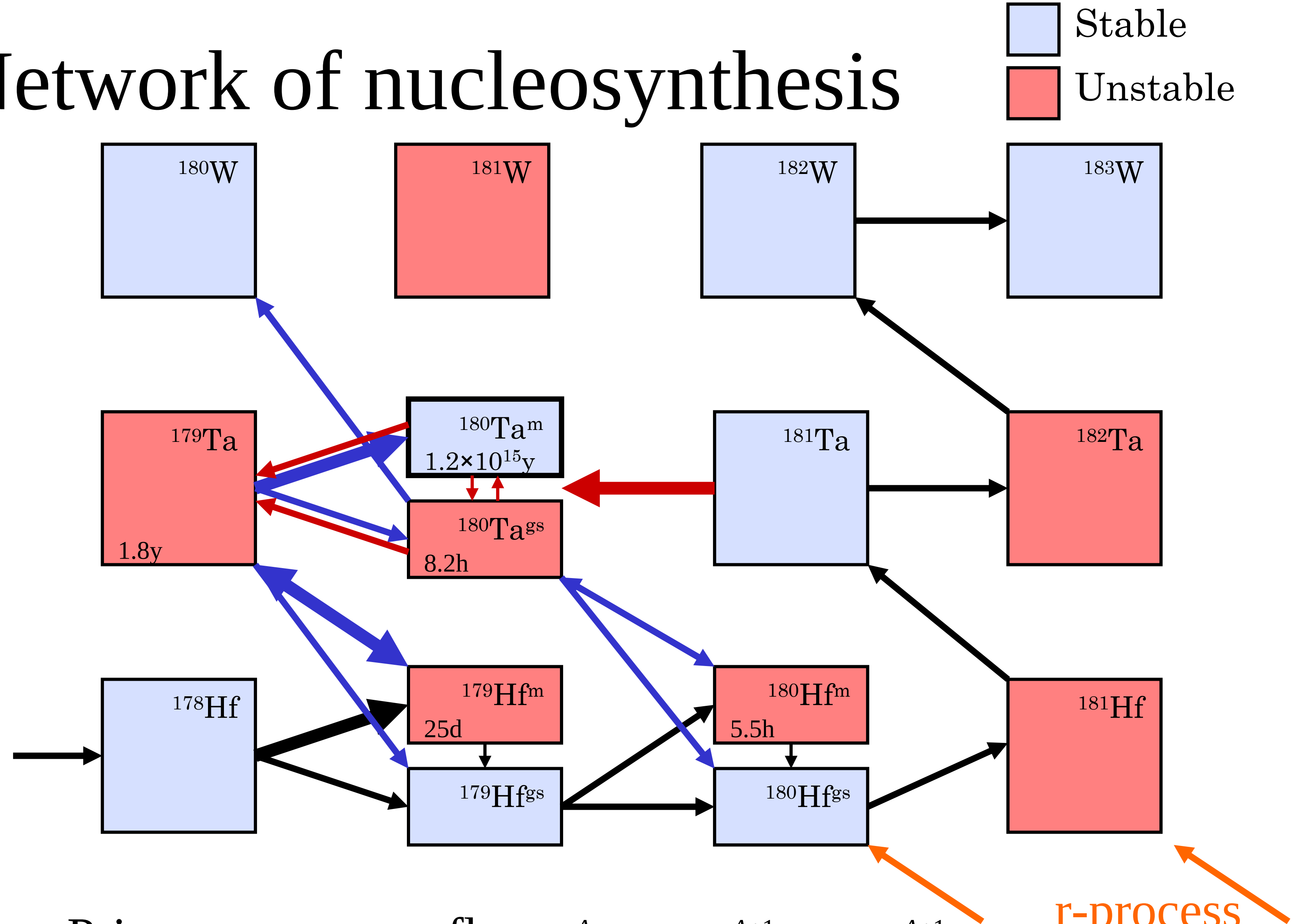

Primary s-process flow $^{A}_{Z}X\,(n,\gamma)\,^{A+1}_{Z}X\,(\beta^{-})\,^{A+1}_{Z+1}X'$

p-process $^{181}Ta(\gamma,n)^{180}Ta(thermal\ equilibrium)^{180}Ta^{m}$

Weak branching s-process $^{179}Hf^{m}(\beta)^{179}Ta(n,\gamma)^{180}Ta^{m}$

Nucleosynthesis of $^{180}Ta^{m}$

- p-process in the pre-supernova phase of massive stars or during their explosions as type-□supernovae

  Temperature ; 1.8 □ $T[10^{9}K]$ □ 3.0

  Peak photon energy ; 200[keV]

  $^{181}Ta(\gamma,n)^{180}Ta$(thermal equilibrium) $^{180}Ta^{m}$

- s-process in the Low-mass AGB star

  Temperature ; 2.9 □ $T[10^{8}K]$ □ 3.3

  (Zs. Nèmeth, F. Käppeler, G. Reffo; 1992)

  Typical neutron energy ; 25[keV]

  $^{179}Hf^{m}(\beta)^{179}Ta(n,\gamma)^{180}Ta^{m}$

$^{181}Ta(\gamma,n)^{180}Ta$

H. Utsunomiya et al., Phys. Rev. C 67, 015807 (2003)

Extra E1 γ-ray strength near Sn

Pygmy Dipole Resonance
N. Paar, D. Vretenar, E. Khan, G. Colò
Rep. Prog. Phys. ***70 691*** *(*2007)

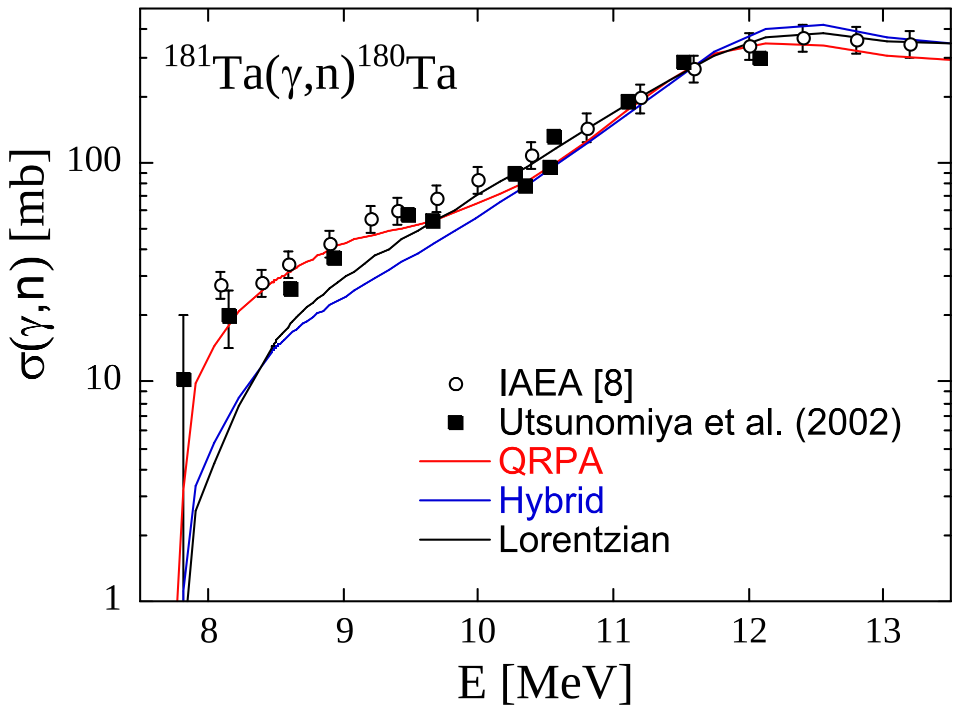

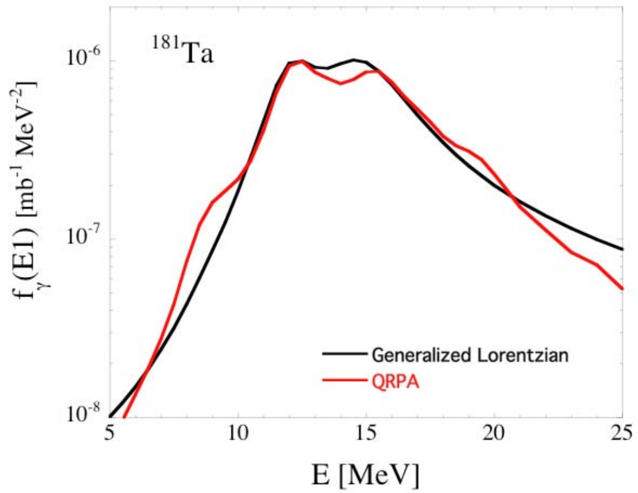

Model calculation of the p-process nucleosynthesis

H. Utsunomiya et al., Phys. Rev. C 67, 015807 (2003)

S. Goriely, ULB

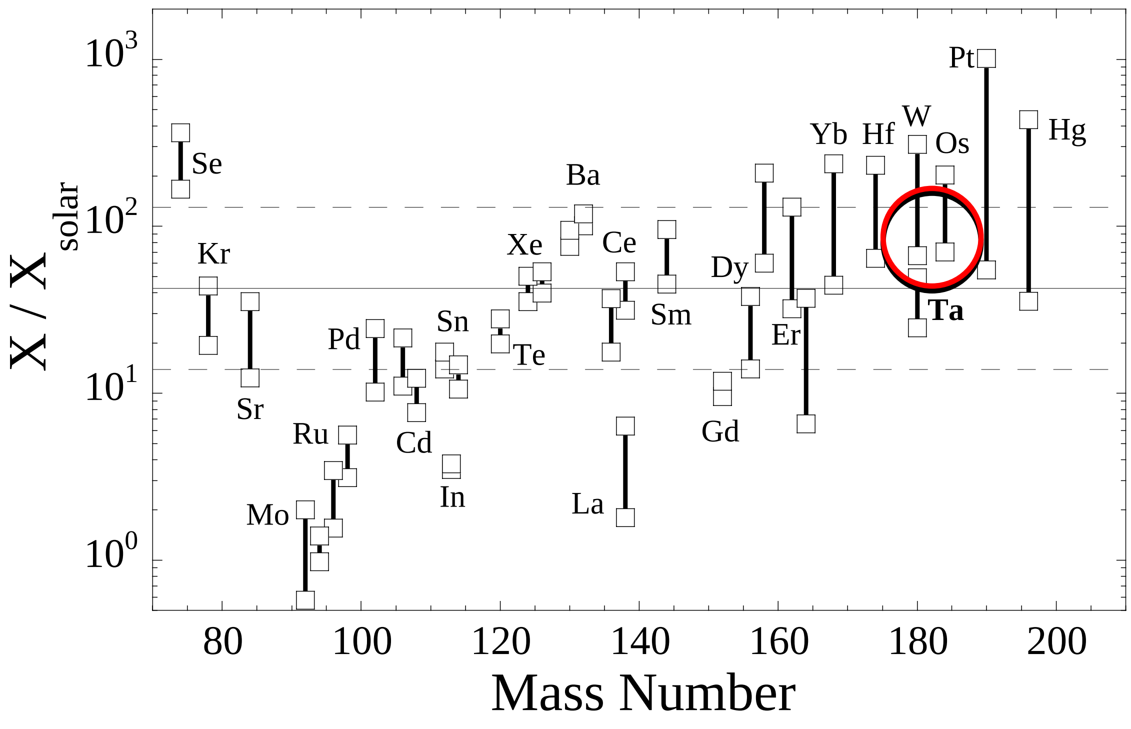

Nuclear Level Density of ^{180}Ta

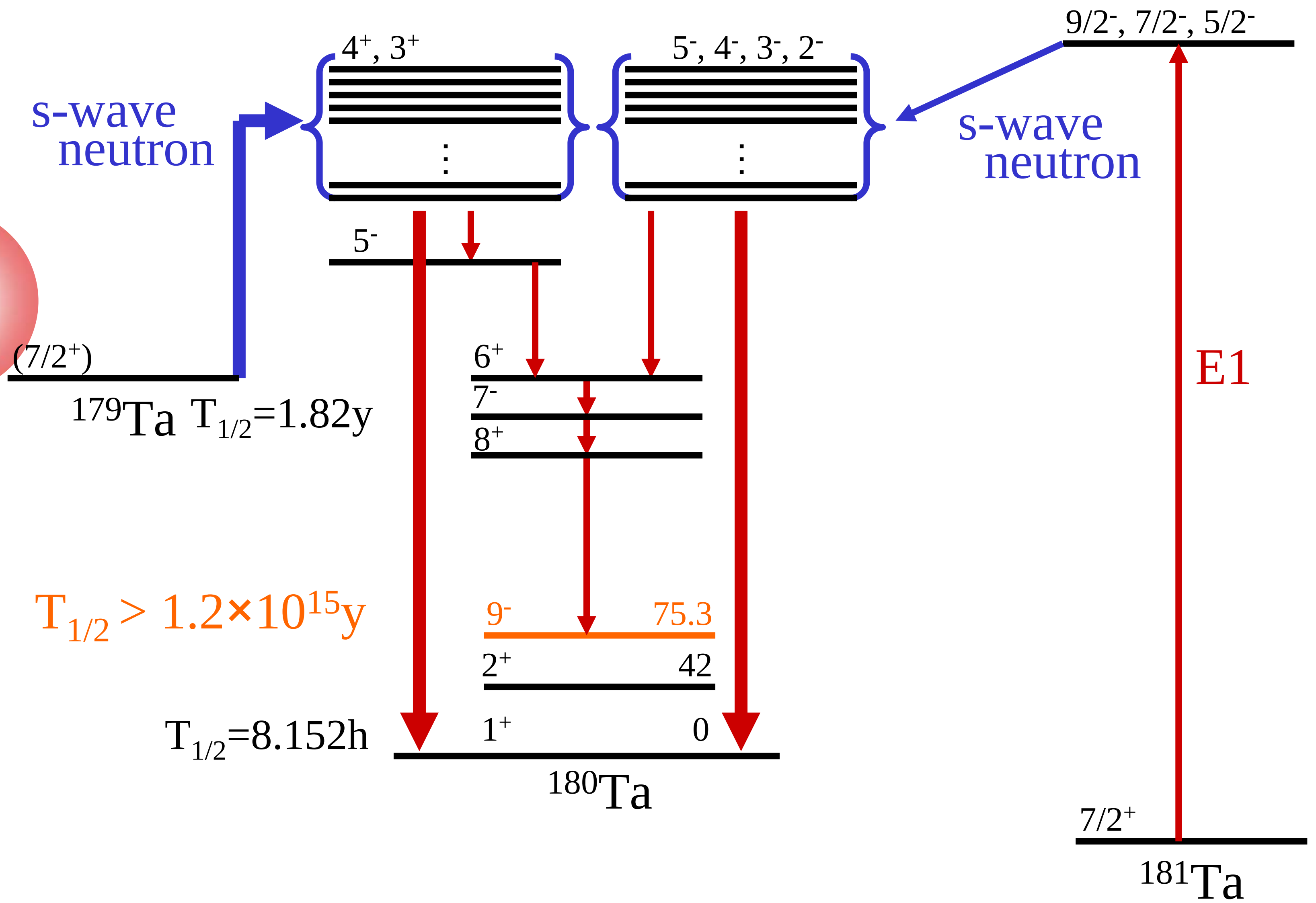

Progress of the reactions

$T_{1/2} > 1.2\times10^{15}$y
$T_{1/2}$=8.152h

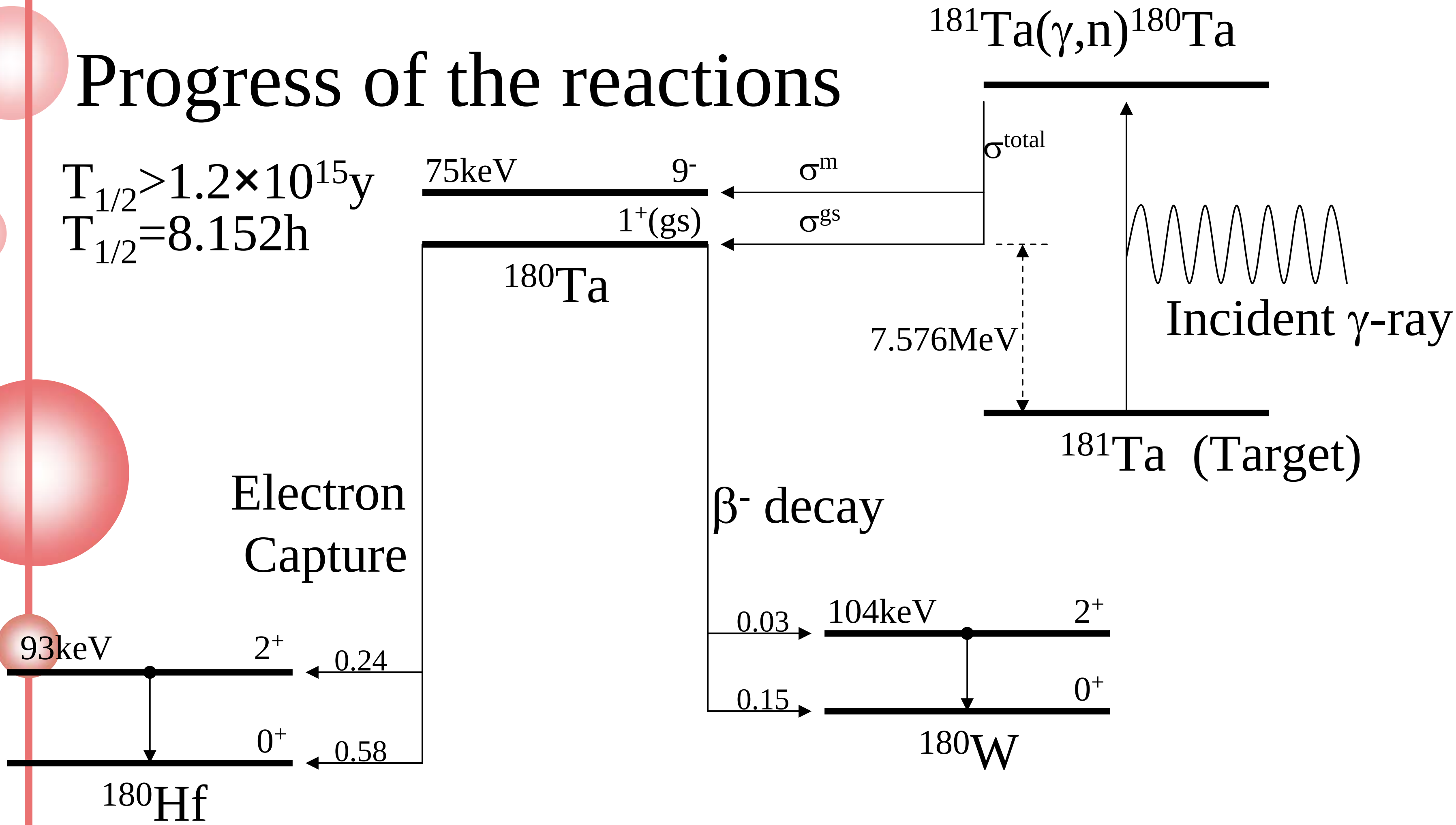

per 1 decay of $^{180}Ta^{gs}$
93keV γ-ray 4.665%
55.8keV $K_{\alpha1}$ 33.12%
54.6keV $K_{\alpha2}$ 19.20%

$$\sigma^{m} = \sigma^{total} - \sigma^{gs}$$

Experimental Set-up

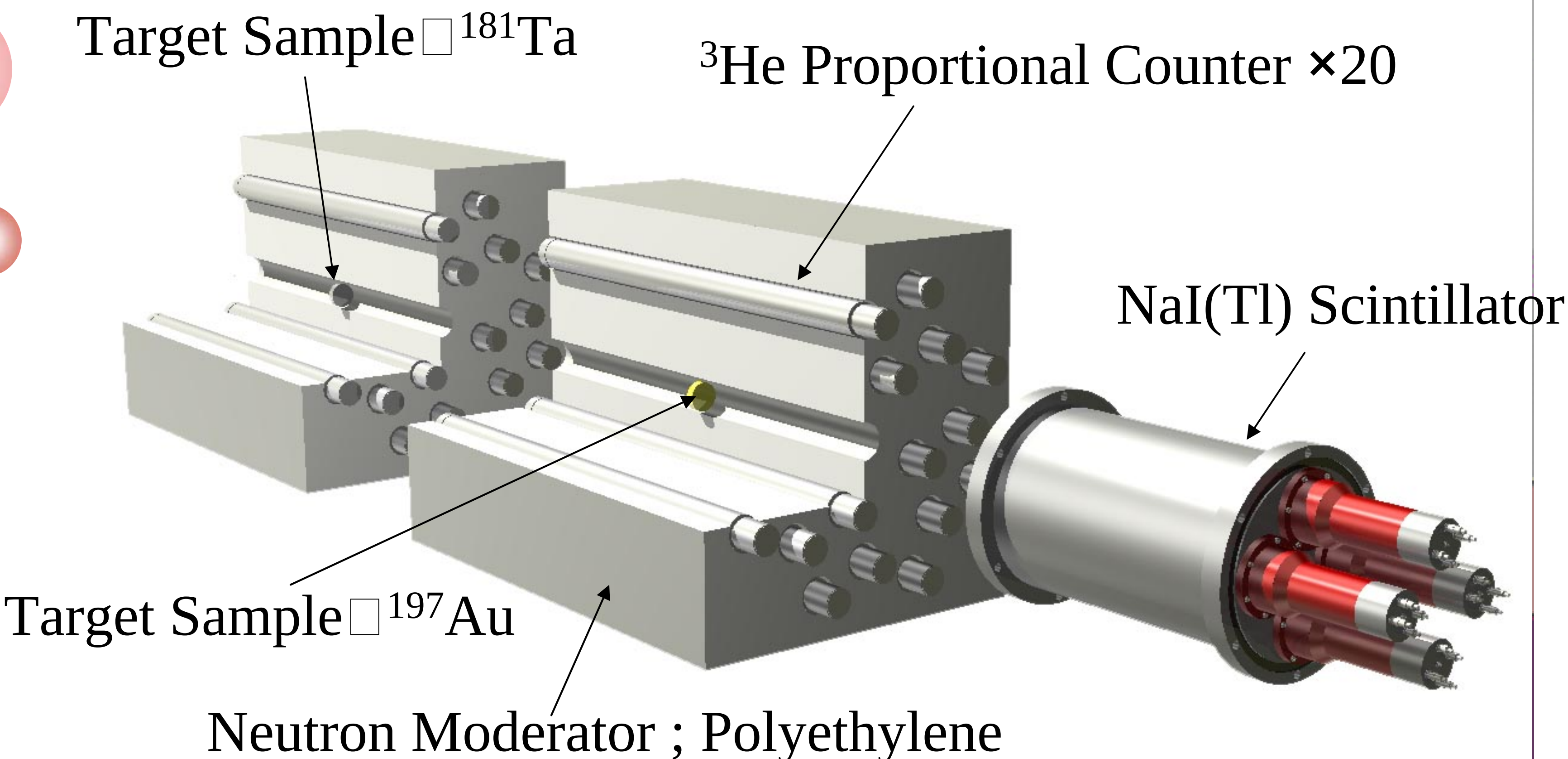

$^{180}Ta^{gs} \rightarrow {}^{180}Hf$ □Electron Capture

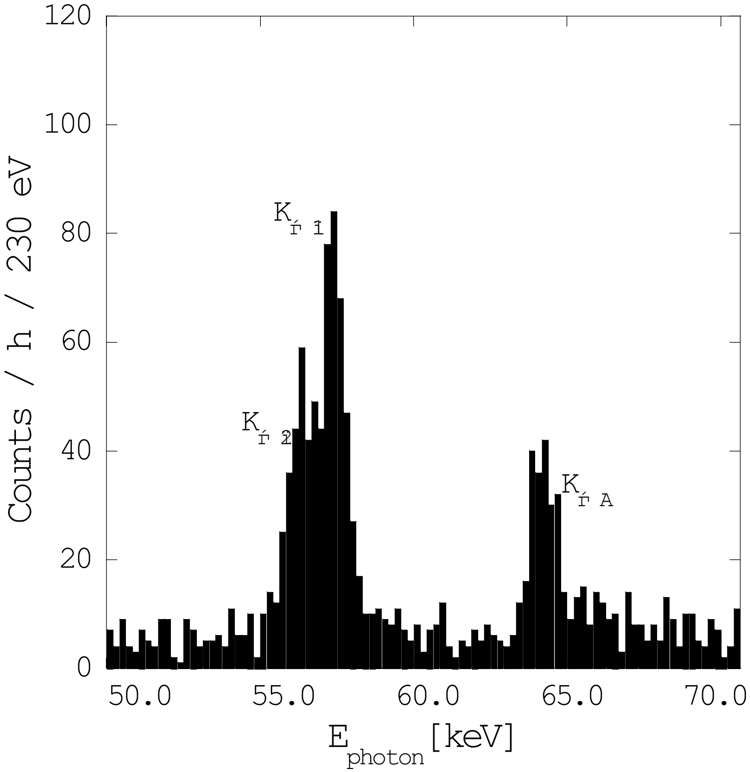

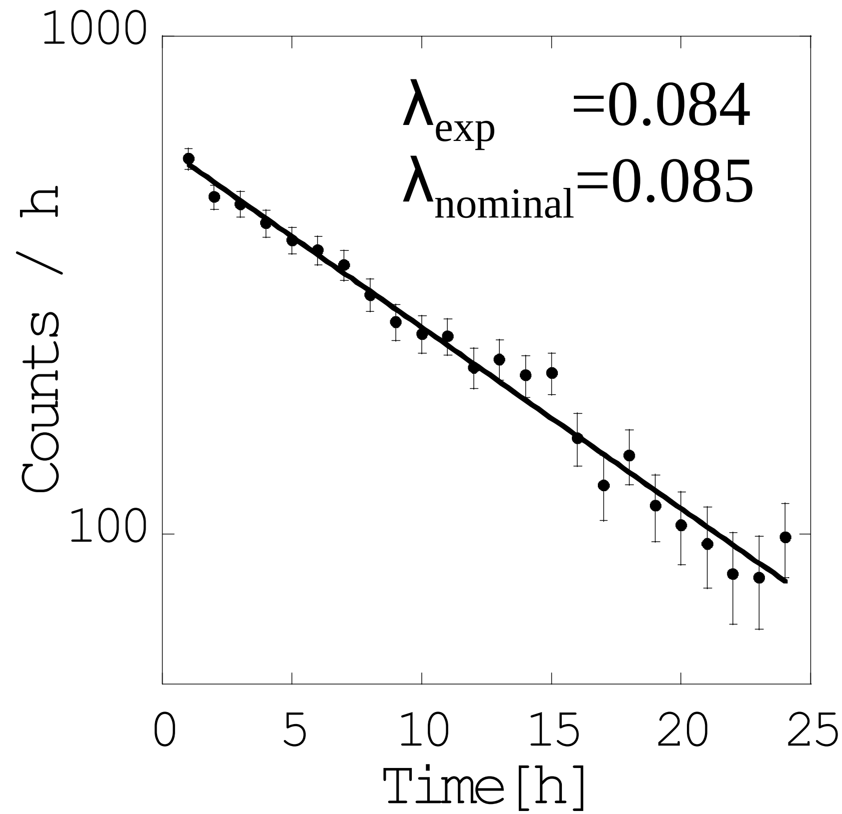

Experimental results, and comparison with theoretical models

Goko et al. Phys. Rev. Lett. 96, 192501 (2006)

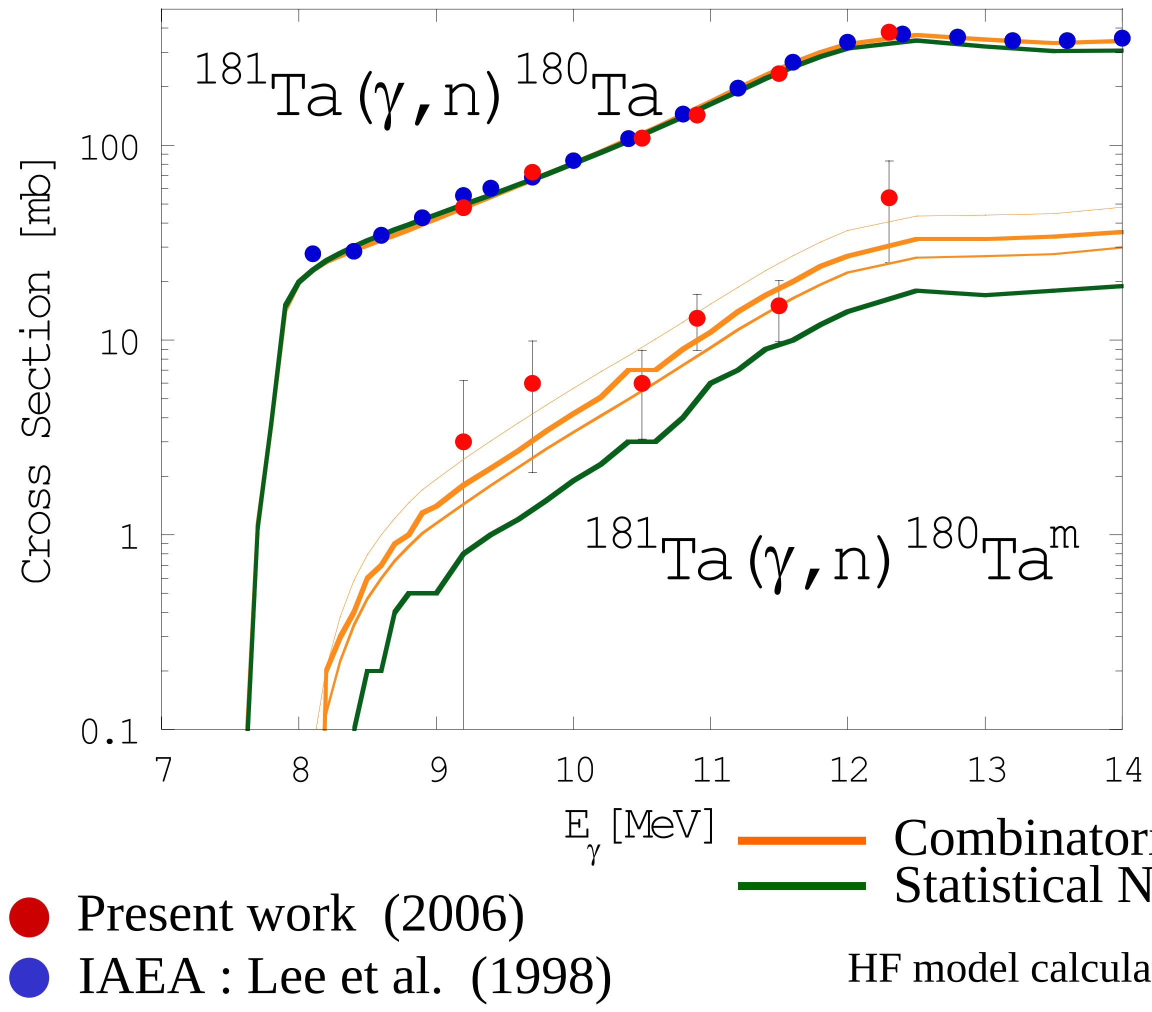

Systematic uncertainties 10□26%

HF model calculations by S.Goriely (ULB)

$^{179}Ta(n,\gamma)^{180}Ta^m$
for the s-process $^{180}Ta^m$ production

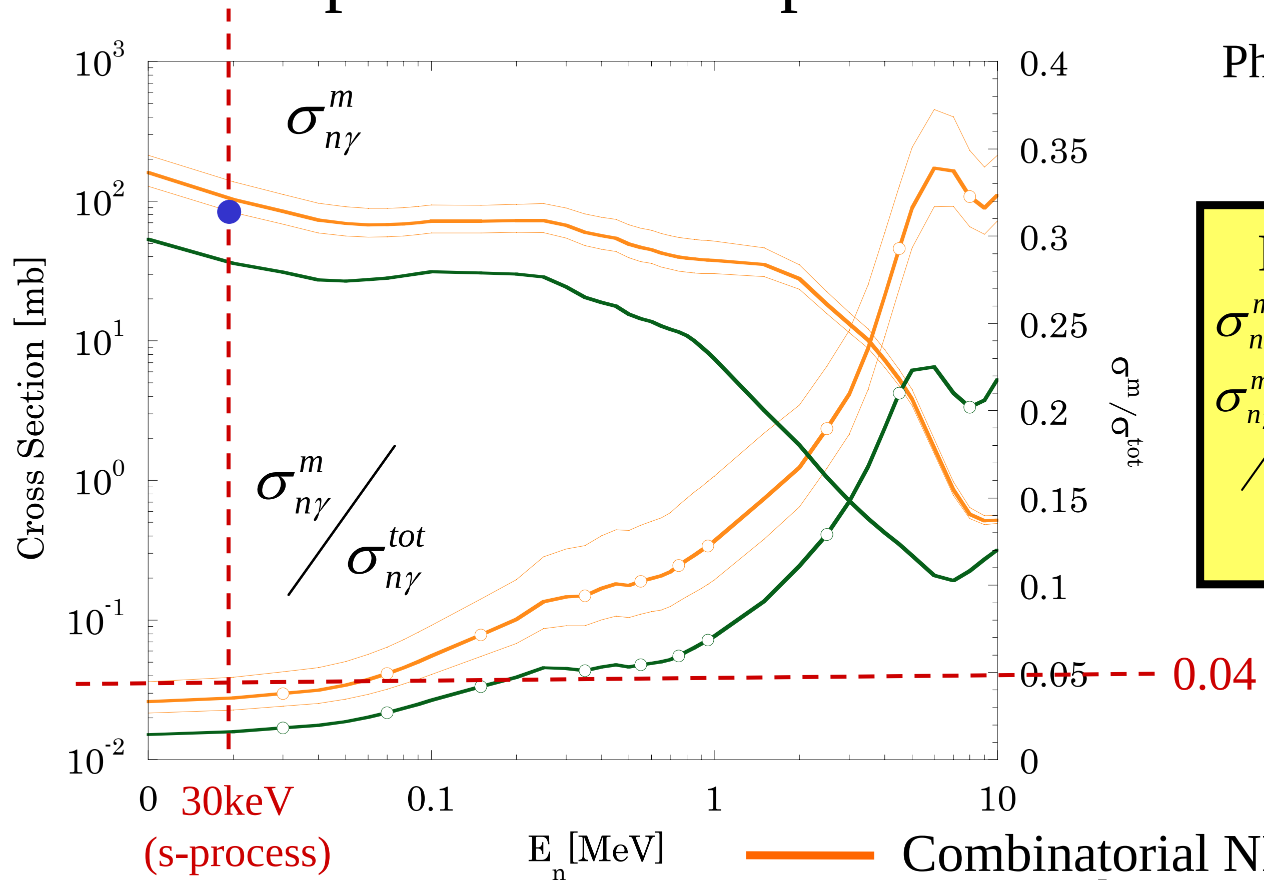

HF model calculations by S.Goriely (ULB)

Goko et al.
Phys. Rev. Lett. 96, 192501 (2006)

Present results

$\sigma_{n\gamma}^{m} = 90 \pm 22 mb$

$\sigma_{n\gamma}^{m} / \sigma_{n\gamma}^{tot} = 0.04 \pm 0.01$

at 30 keV

Previous Predictions

σ^m □ ● 44mb (Zs. Nèmeth, F.Käppeler, G.Reffo ;1992)

σ^m/σ^{tot} □ 0.02□0.09 (K.Yokoi, K.Takahashi ;1983)

0.043±0.008 (Zs. Nèmeth, F.Käppeler, G.Reffo ;1992)

Radiative neutron capture - ${}^{A}X(n,\gamma)^{A+1}X$

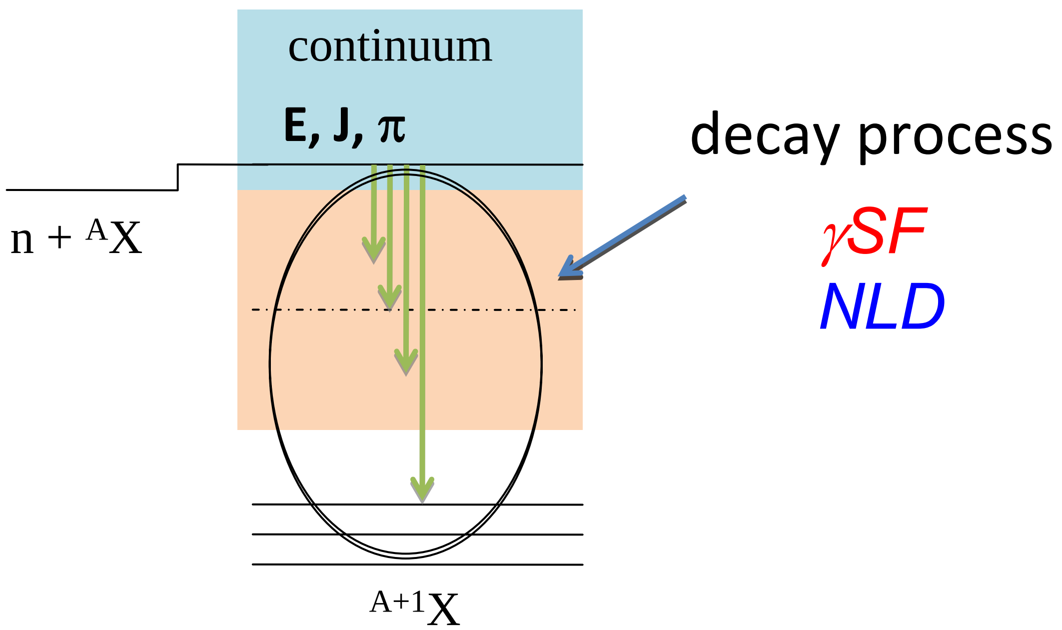

Hauser-Feshbach model cross section for $^{A}X(n,\gamma)^{A+1}X$

$$\sigma_{n\gamma}(E) = \frac{\pi}{k_n^2}\sum_{J,\pi} g_J \frac{T_\gamma(E,J,\pi)\, T_n(E,J,\pi)}{T_{tot}} \cong \frac{\pi}{k_n^2}\sum_{J,\pi} g_J T_\gamma(E,J,\pi)$$

$$T_{tot} \approx T_n(E,J,\pi)$$

Total γ transmission coefficient

After integrating over J and π

$$T_\gamma(E,J,\pi) = \sum_{\nu,X,\lambda} T^{\nu}_{X\lambda}(\varepsilon_\gamma) + \sum_{X,\lambda}\int T_{X\lambda}(\varepsilon_\gamma)\,\rho(E-\varepsilon_\gamma)\,d\varepsilon_\gamma$$

X=E, M

λ=1, 2, …

γ-ray strength function

$$T_{X\lambda}(\varepsilon_\gamma) = 2\pi\varepsilon_\gamma^{2\lambda+1} f_{X\lambda}(\varepsilon_\gamma)\downarrow$$

nuclear level density

$$\rho(E-\varepsilon_\gamma)$$

neutron resonance spacing

low-lying levels

(n,γ) and (γ,n) are interconnected through the γ-ray strength function and the nuclear level density in the Hauser-Feshbach model.

Radiative neutron capture

$^{A}X(n,\gamma)^{A+1}X$

$n+{}^{A}X$

$$f_{X\lambda}(\varepsilon_\gamma)\downarrow = \varepsilon_\gamma^{-(2\lambda+1)}\frac{\langle \Gamma_{X\lambda}(\varepsilon_\gamma)\rangle}{D_\ell}$$

$$\varepsilon_\gamma < S_n$$

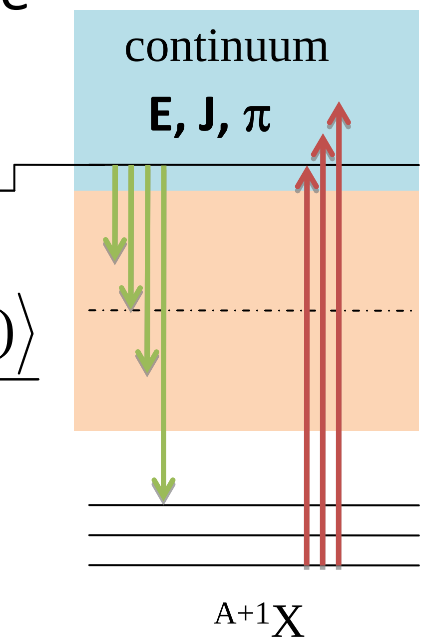

Photoneutron emission

$^{A+1}X(\gamma,n)^{A}X$

$$f_{X\lambda}(\varepsilon_\gamma)\uparrow = \frac{\varepsilon_\gamma^{-2\lambda+1}}{(\pi\hbar c)^2}\frac{\langle \sigma_{X\lambda}^{abs}(\varepsilon_\gamma)\rangle}{2\lambda+1}$$

$$\varepsilon_\gamma > S_n$$

Brink Hypothesis

$$f_{X\lambda}(\varepsilon_\gamma)\uparrow \cong f_{X\lambda}(\varepsilon_\gamma)\downarrow$$

Experimental determination of γ-ray strength function

$^{A-1}X(n, \gamma)^{A}X$

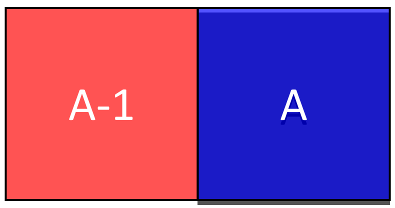

Statistical model calculation of $^{A-1}X(n, \gamma)^{A}X$ cross sections with experimental γSF

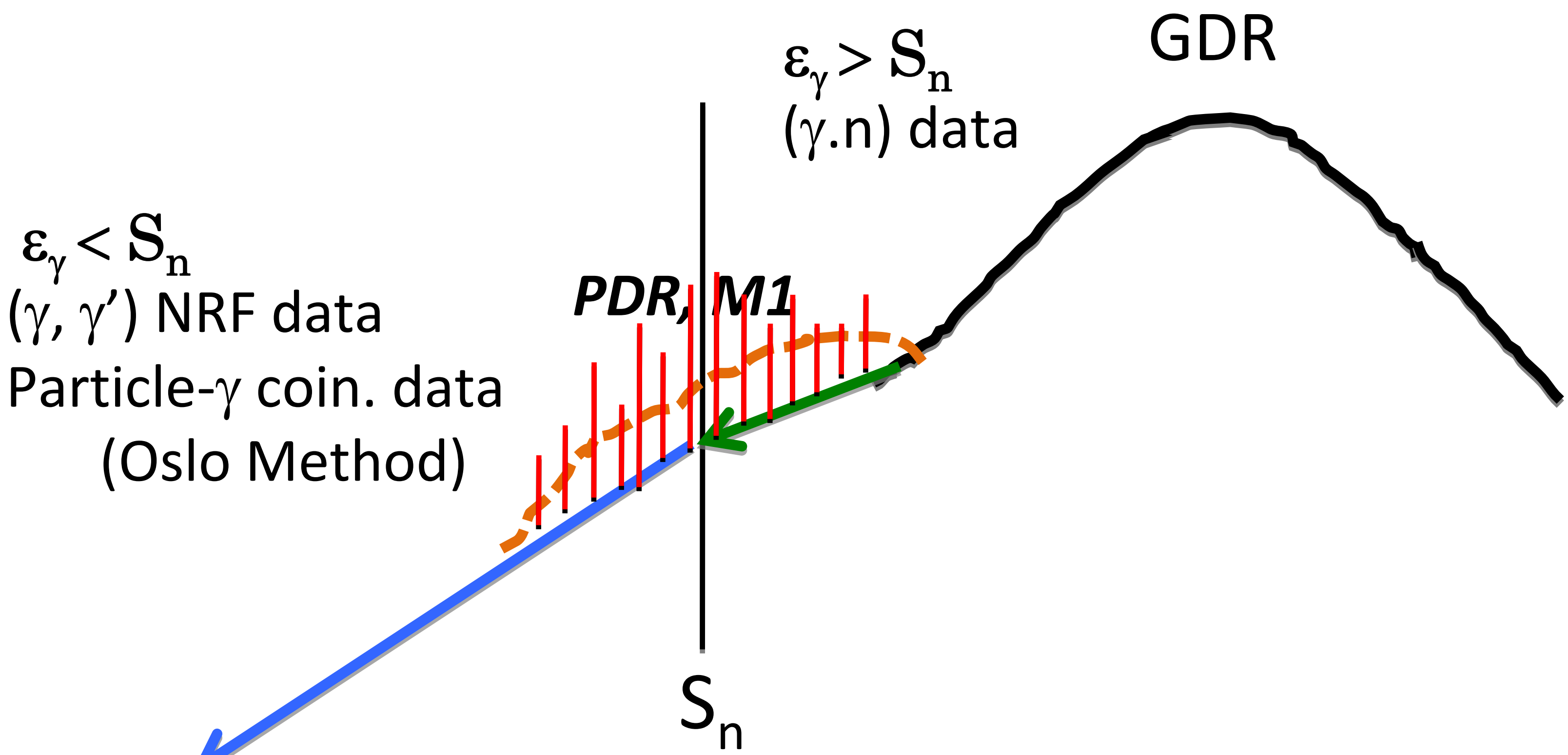

Theoretical extrapolation of γ-ray strength function

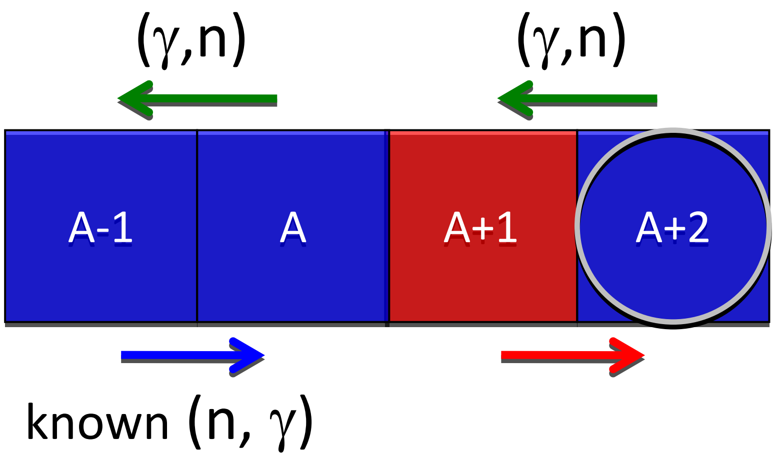

Statistical model calculation of $^{A+1}X(n,\gamma)^{A+2}X$ cross sections with experimentally-constrained γSF

1. $\varepsilon_\gamma > S_n$
(γ.n) data

2. $\varepsilon_\gamma < S_n$
Extrapolation by
<u>microscopic model</u>

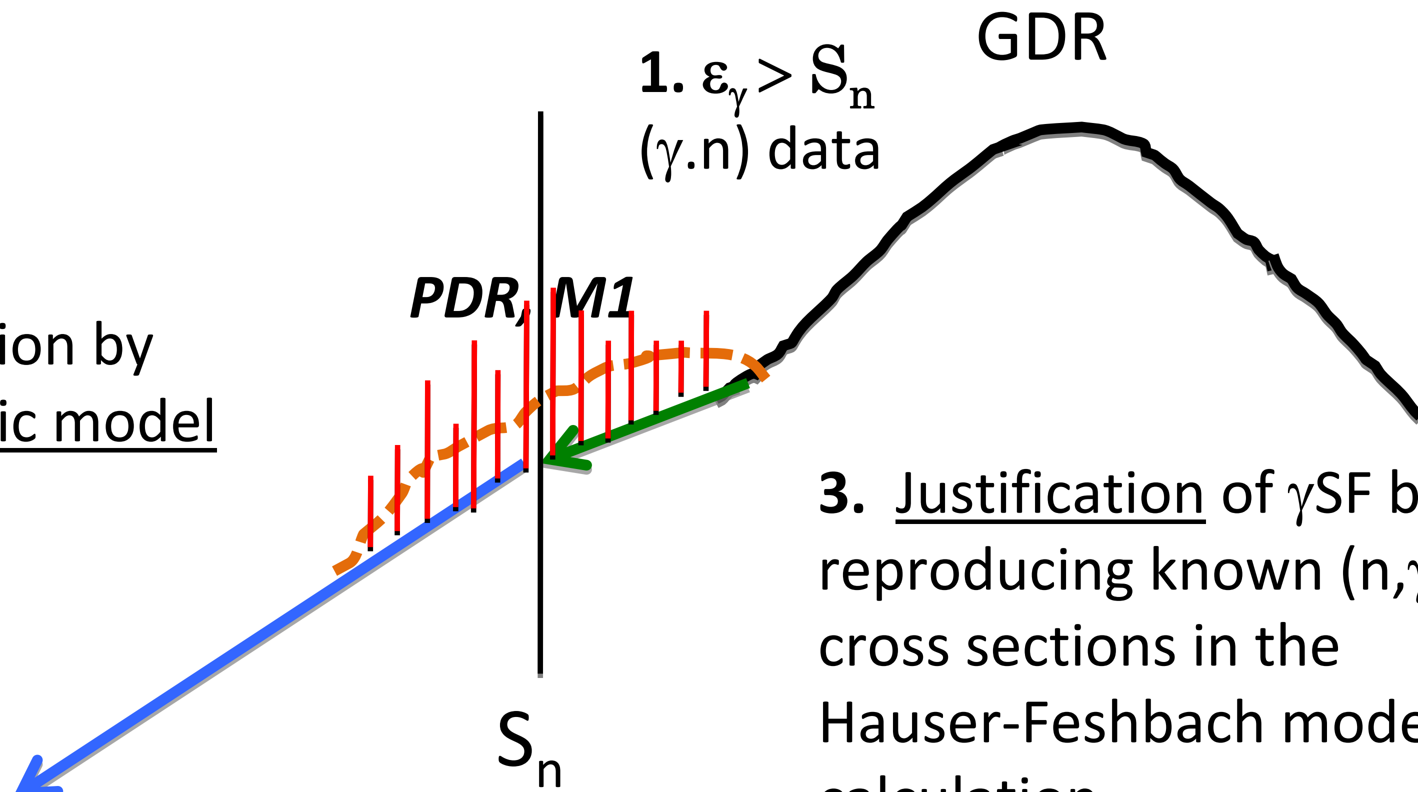

3. <u>Justification</u> of γSF by reproducing known (n,γ) cross sections in the Hauser-Feshbach model calculation

γ-ray Strength Function Method

H. Utsunomiya et al., Phys. Rev. C 80, 055806 (2009)

Indirect determination of (n, γ) cross sections for unstable nuclei based on a unified understanding of (γ,n) and (n, γ) reactions through the γ-ray strength function

The best understanding of the γ SF with PDR and M1 resonance is obtained by integrating

- (γ, n) data
- (γ, γ') NRF data
- Particle-γ coin. data , Oslo Method
- Existing (n, γ) data

Applications of the γ-ray Strength Function Method

1. Nuclear Astrophysics

s-process branch-point nuclei: unstable nuclei along the line of β-stability

F. Käppeler *et al.*, Rev. Mod. Phys. **83**, 157 (2011)

63Ni, 79Se, 81Kr, 85Kr, 95Zr, 147Nd, 151Sm, 153Gd, 185W

2.Nuclear Data for Nuclear Engineering

nuclear transmutation of long-lived fission product

79Se, 93Zr, 107Pd etc.

Applications

LLFP (long lived fission products)
nuclear waste

Astrophysical significance

Present (γ,n) measurements

Existing (n,γ) data

(n,γ) c.s. to be deduced

H. Utsunomiya et al., PRC80 (2009)

H.U. et al., PRC82 (2010)

H.U. et al., PRL100(2008)
PRC81 (2010)

F. Kitatani, Ph.D. thesis,
to be published

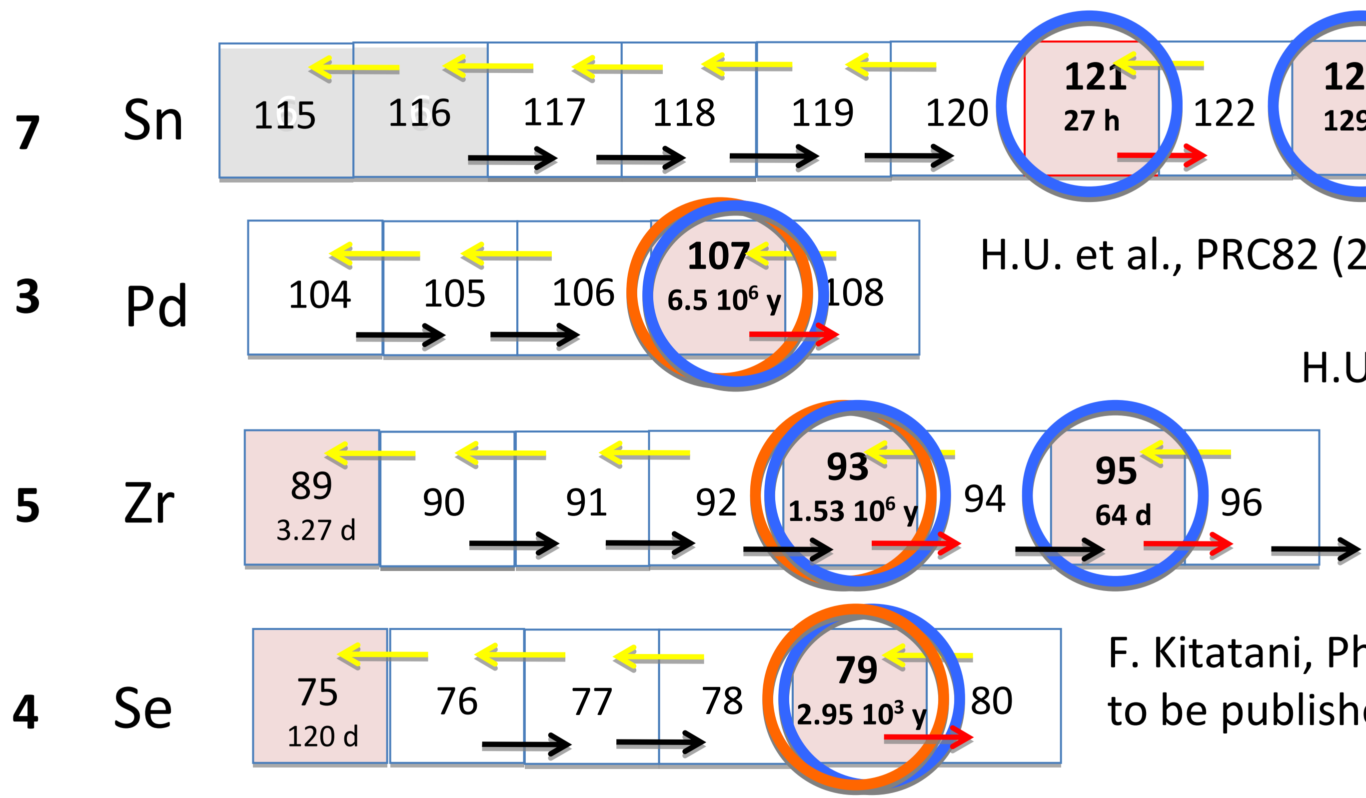

H.U. et al., PRC88 (2013)

6

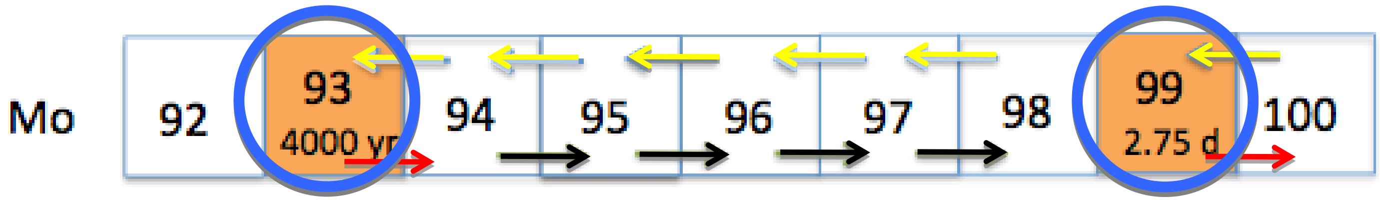

In collaboration with Univ. Oslo etc.

5

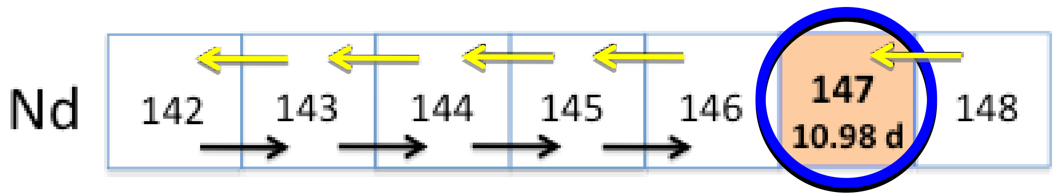

In collaboration with ELI-NP etc.

7

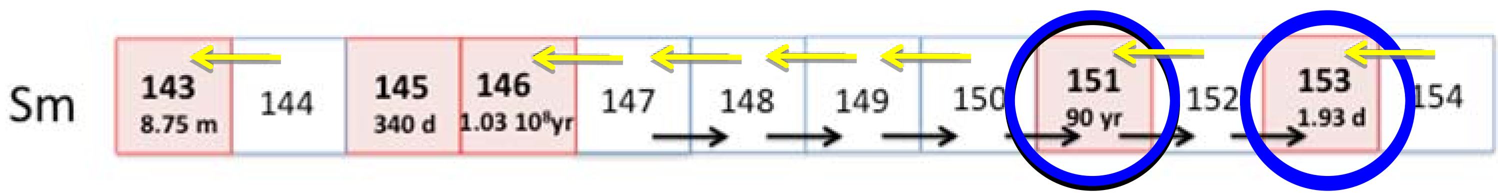

Sn isotopes

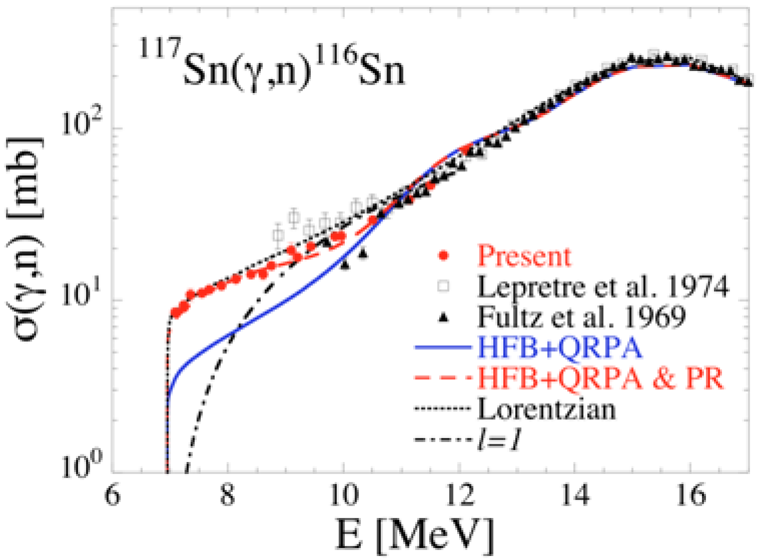

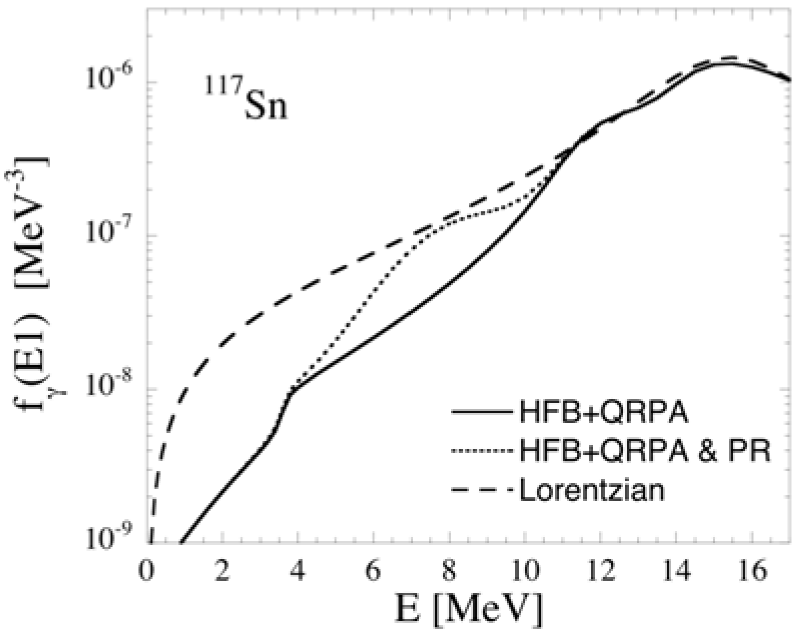

HFB+QRPA E1 strength supplemented with a pygmy E1 resonance in Gaussian shape

$E_o \approx 8.5$ MeV, $\Gamma \approx 2.0$ MeV, $\sigma_o \approx 7$ mb

 1% of TRK sum rule (E1 strength)

γ**SF** for Sn isotopes

(γ,n) data

H. Utsunomiya et al., PRC84 (2011)

Oslo data

(3He, αγ), (3He, 3He' γ)

Toft et al., PRC 81 (2010); PRC 83 (2011)

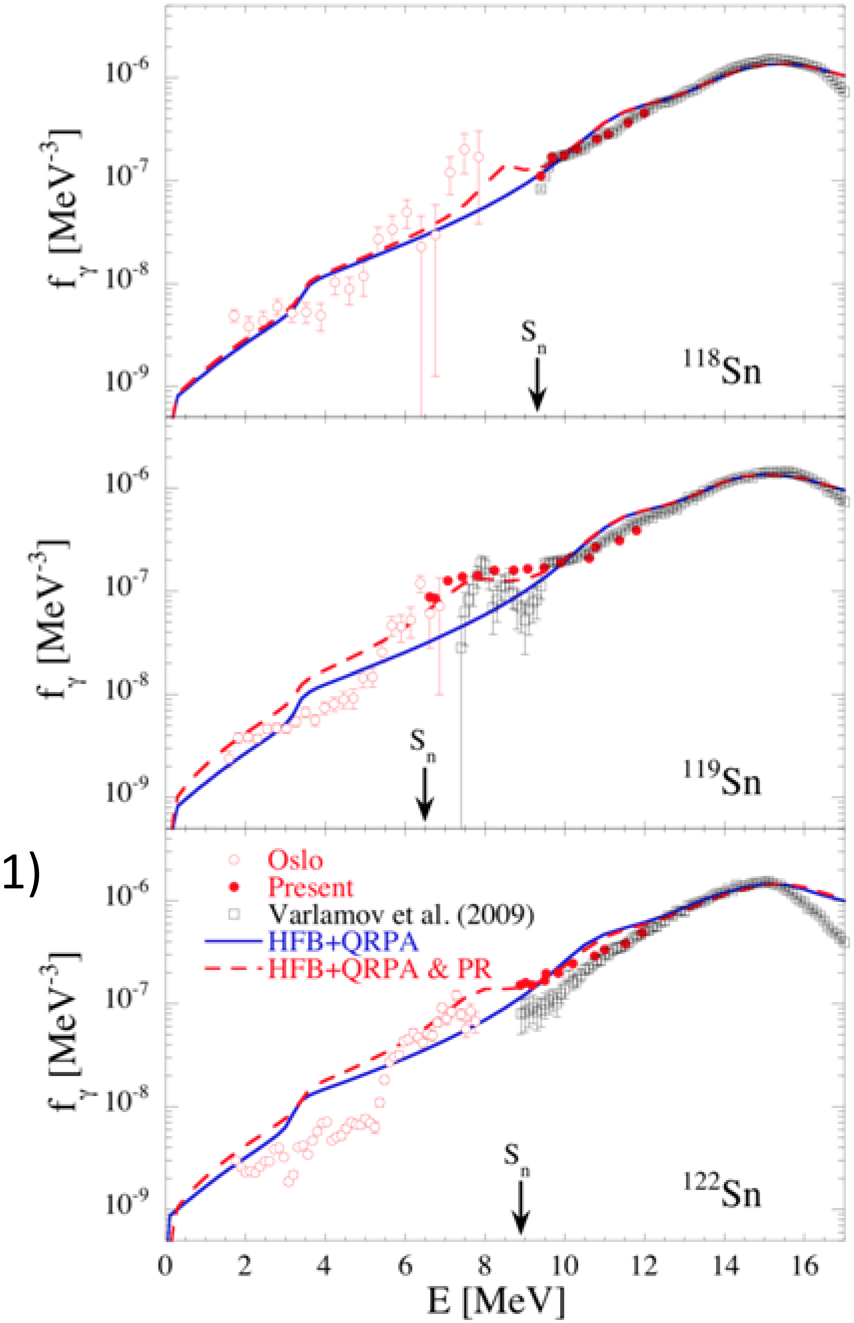

(n,γ) CS for Sn isotopes

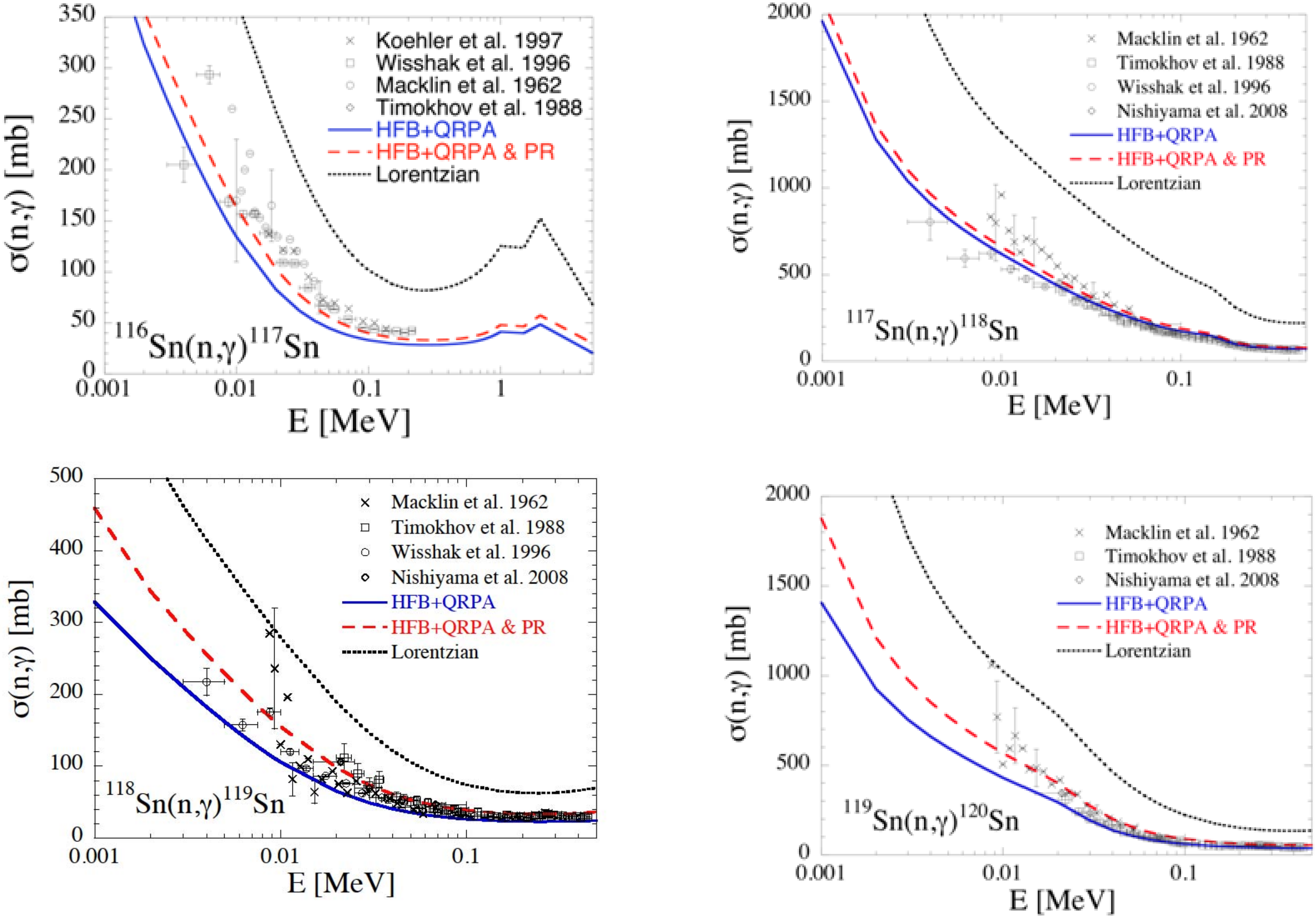

(n,γ) CS for unstable Sn isotopes

$^{121}Sn[T_{1/2}=27\ h]$

$^{123}Sn[T_{1/2}=129\ d]$

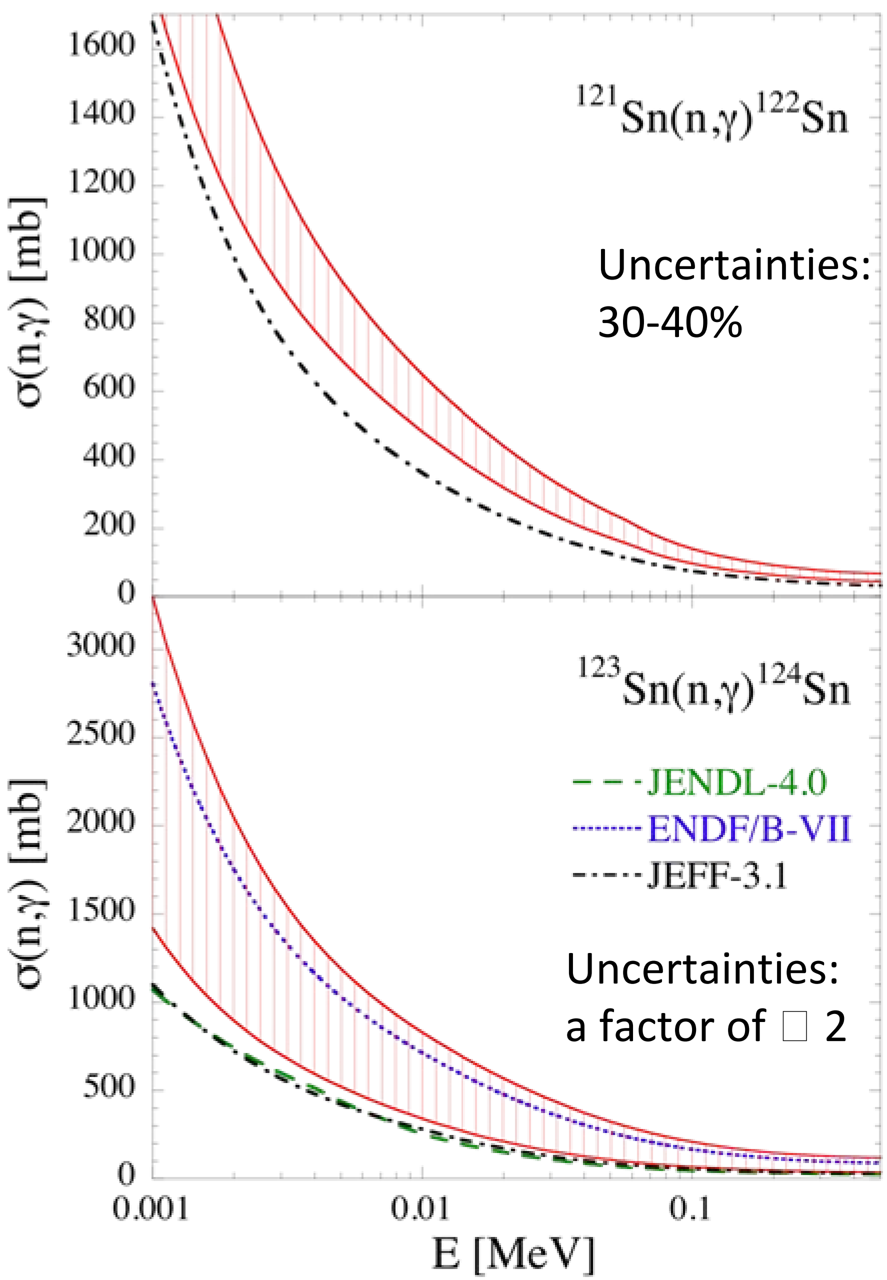

Mo isotopes

(γ,n) data

H. Utsunomiya et al., PRC 88 (2013)

Oslo data

(3He, αγ□, (3He, 3He’γ□

M. Guttormsen et al., PRC71 (2005)

(γ,γ’) data

G. Rusev et al., PRC77 (2008)

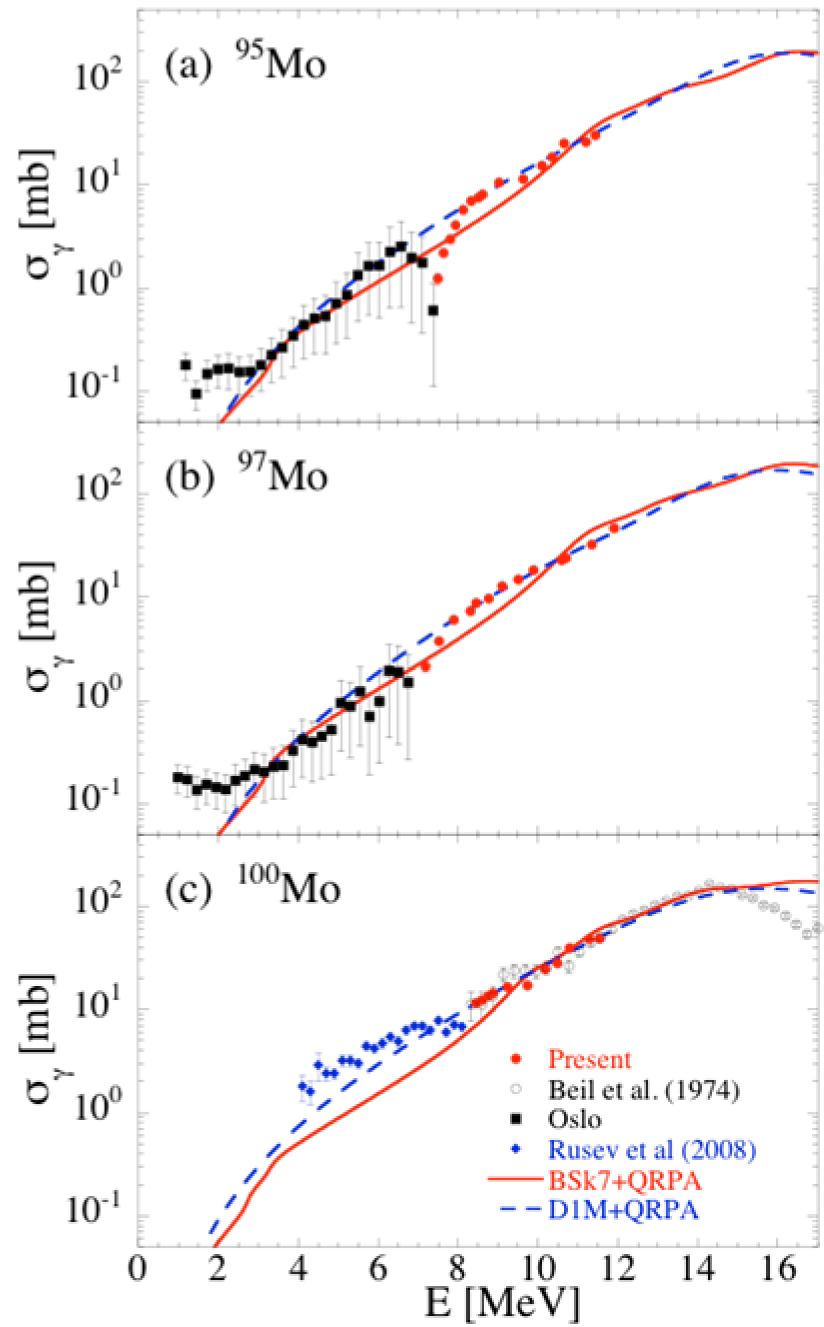

(n,γ) CS for Stable Mo isotopes

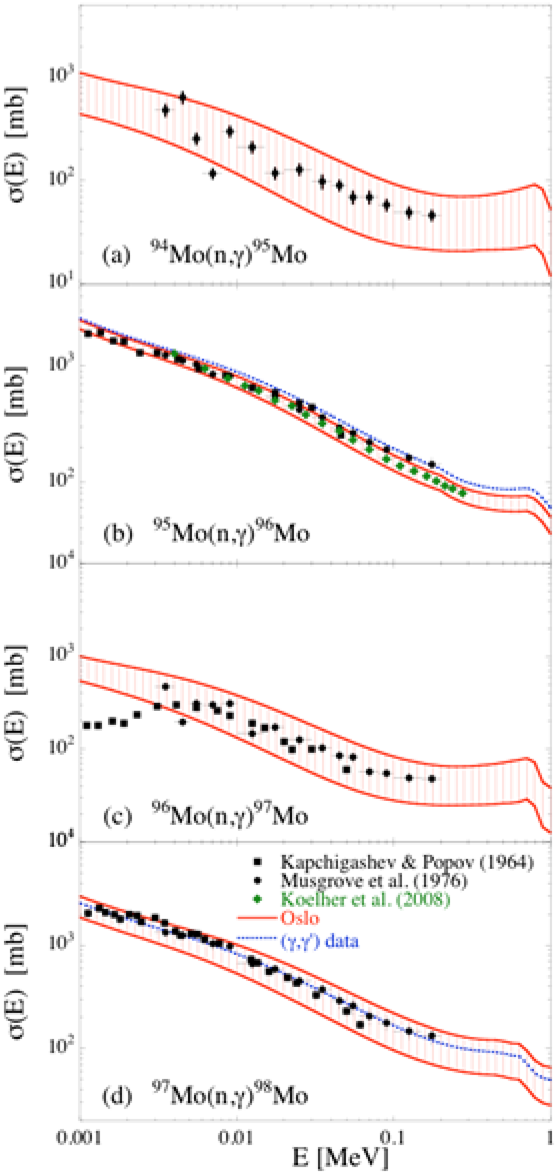

(n,γ) CS for Unstable Mo isotopes

^{93}Mo

$T_{1/2}$=4000 yr

^{99}Mo

$T_{1/2}$=2.75 d

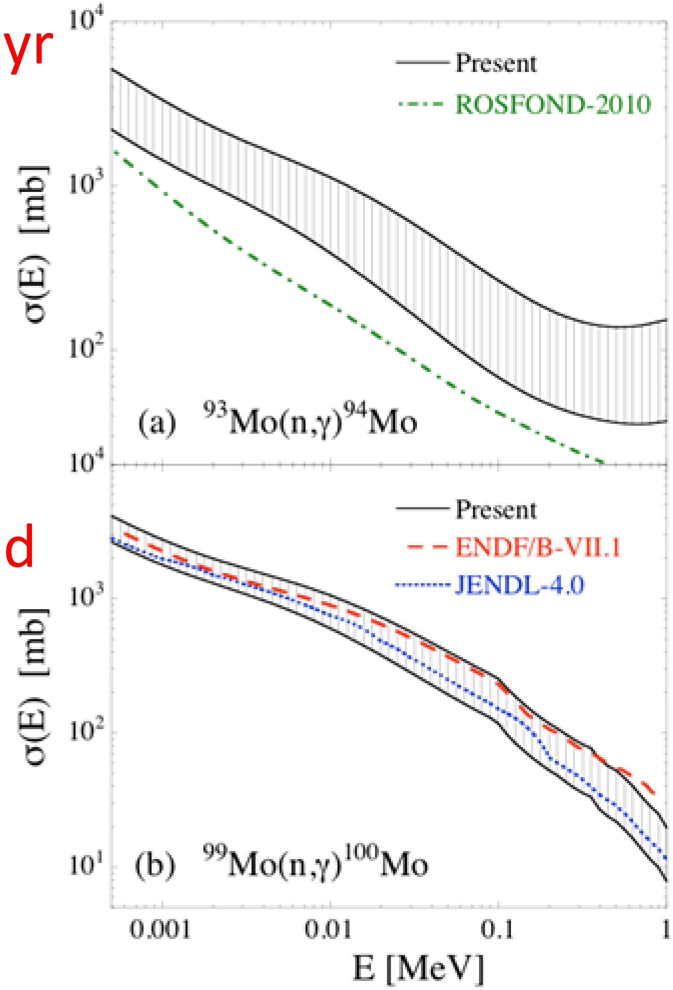

(γ,n) cross sections for Nd isotopes

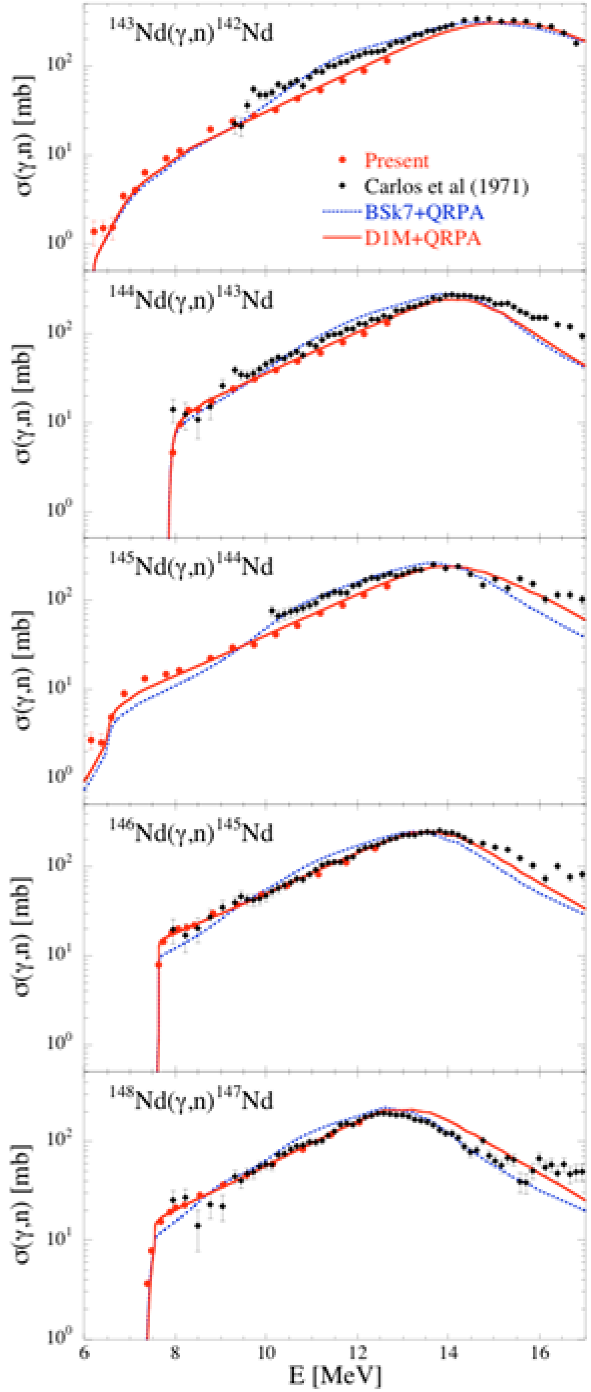

(n,γ) cross sections for Nd isotopes

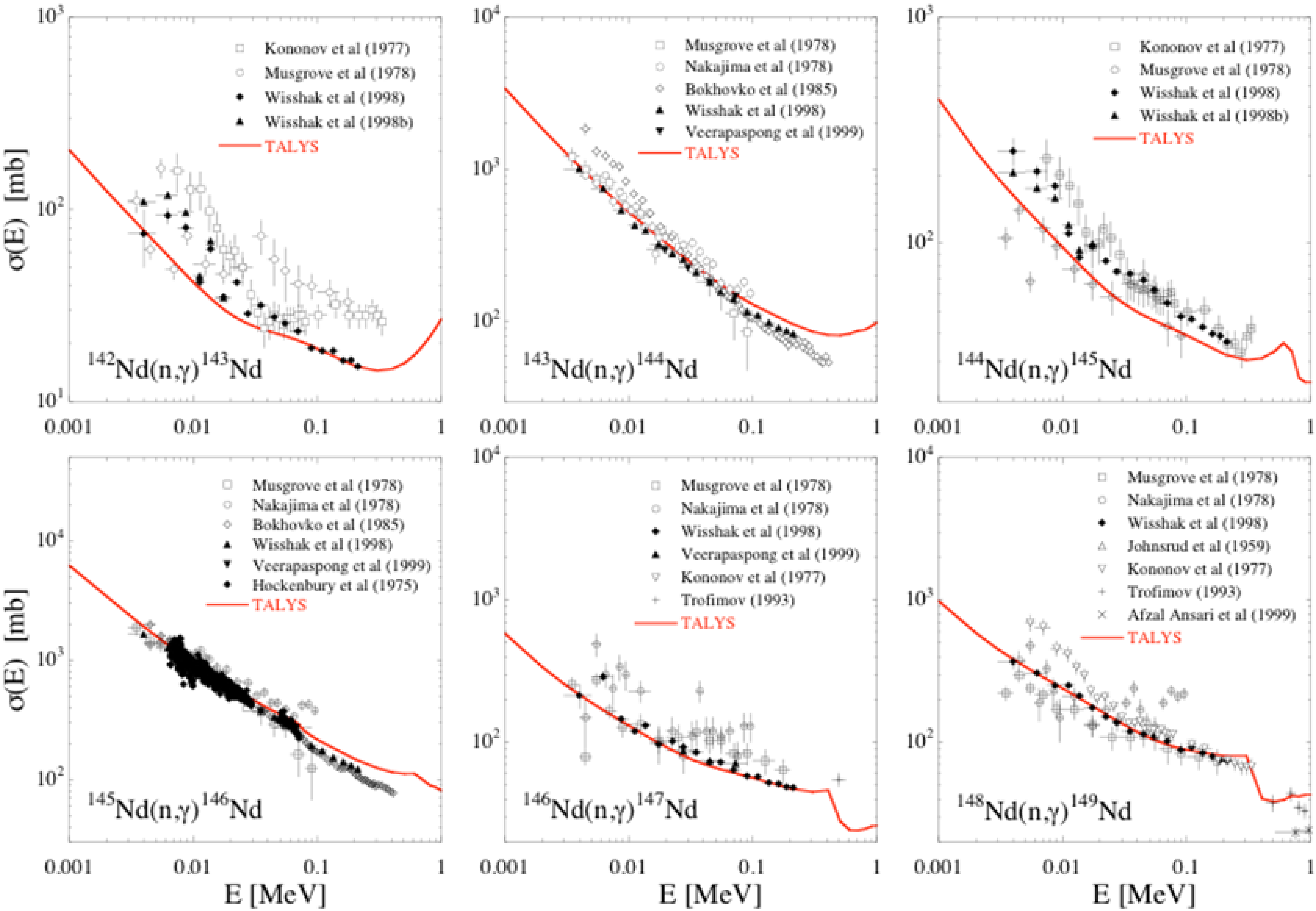

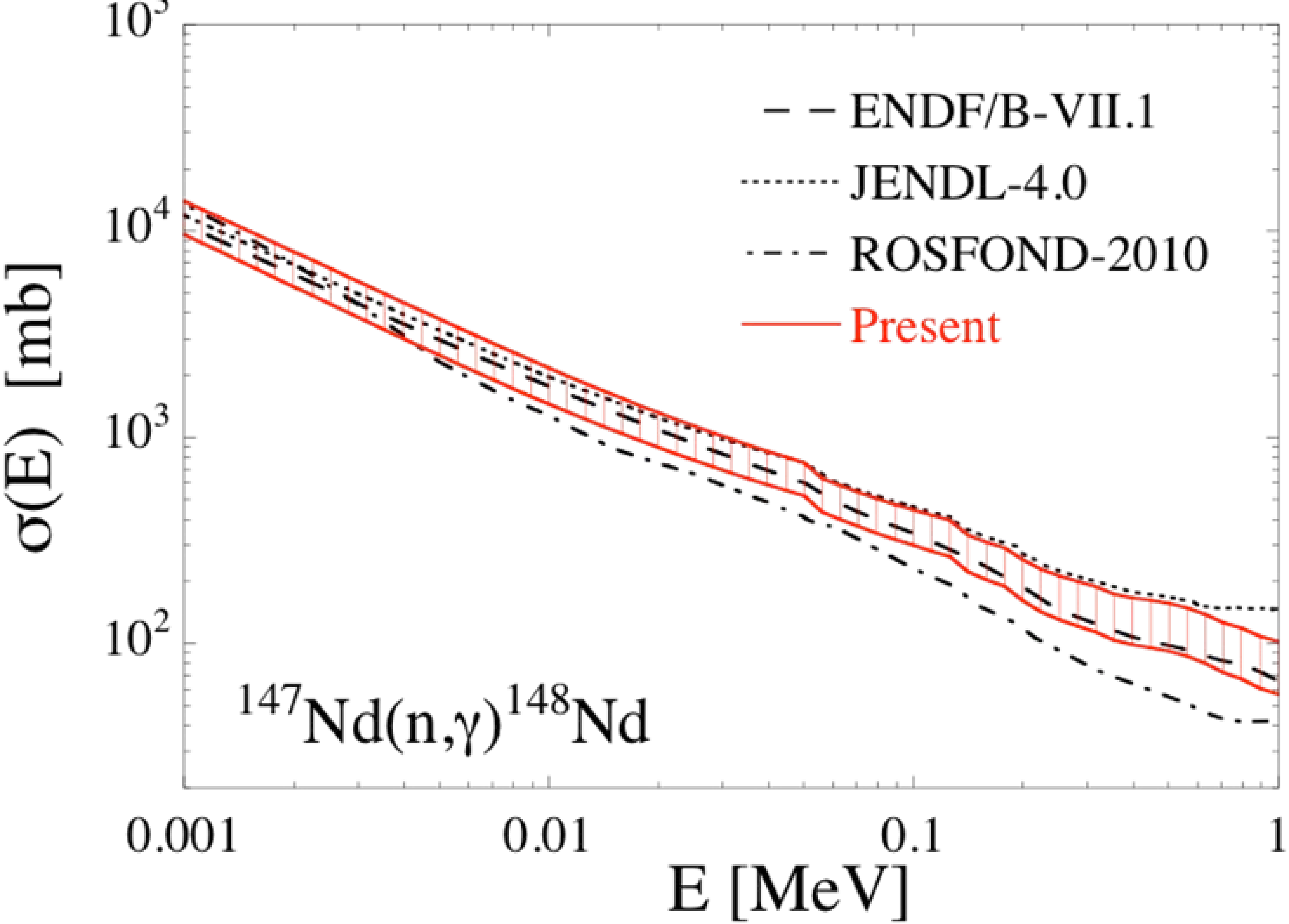

ENDF/B-VII.1
JENDL-4.0
ROSFOND-2010
Present
$^{147}Nd(n,\gamma)^{148}Nd$
10^5
10^4
10^3
10^2
σ(E) [mb]
0.001
0.01
0.1
1
E [MeV]

ELI-NP (Europe)

(Extreme Light Infrastructure- Nuclear Physics)

Magurele-Bucharest, Romania

Approved by the European Commission in 2012

First Experiments in 2018

E_γ = 0.2 -19 MeV

$I_\gamma \geq 10^{11}$ (s^{-1} mm^{-2} $mrad^{-2}$ $0.1\%^{-1}$)

$\Delta E/E \leq 0.5\%$

I. Physics and Experiments with a 4π Neutron Detector

Physics

Rare isotope measurements for the p-process nucleosynthesis

p-nuclei are very rare.

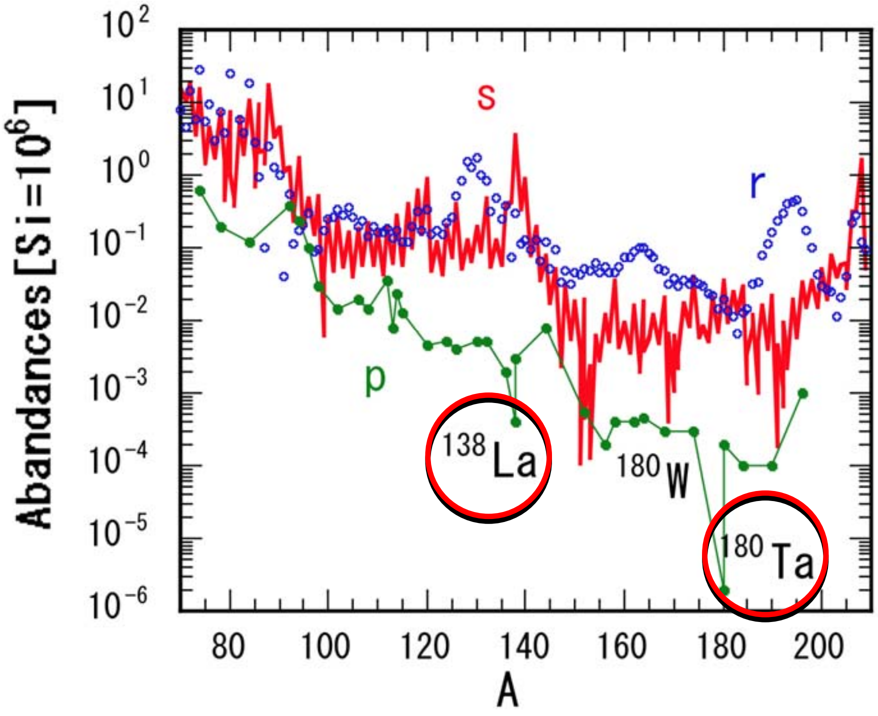

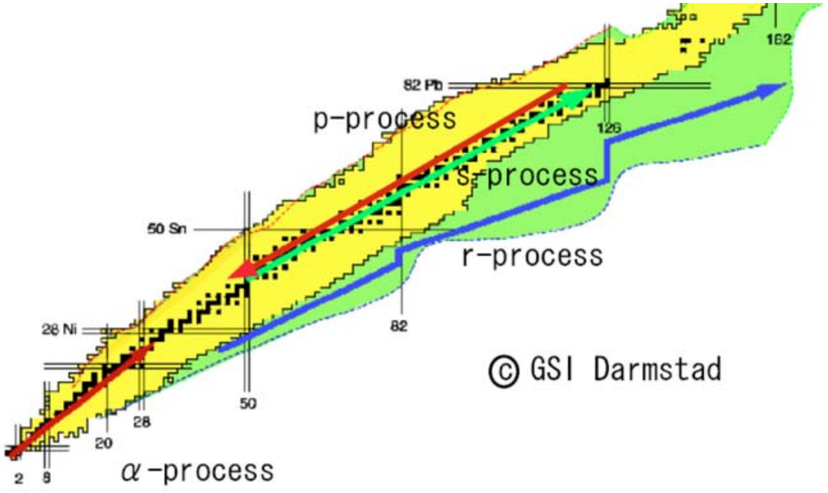

- Highest intensity and monochromatic γ-ray beam
- 1mg samples of rare isotopes

Rarest element
Only naturally-occurring isomer

Production	vs	Destruction
181Ta(γ,n)180Ta		180Ta(γ,n)179Ta
139La(γ,n)138La		138La(γ,n)137La
measured!		Not so ever

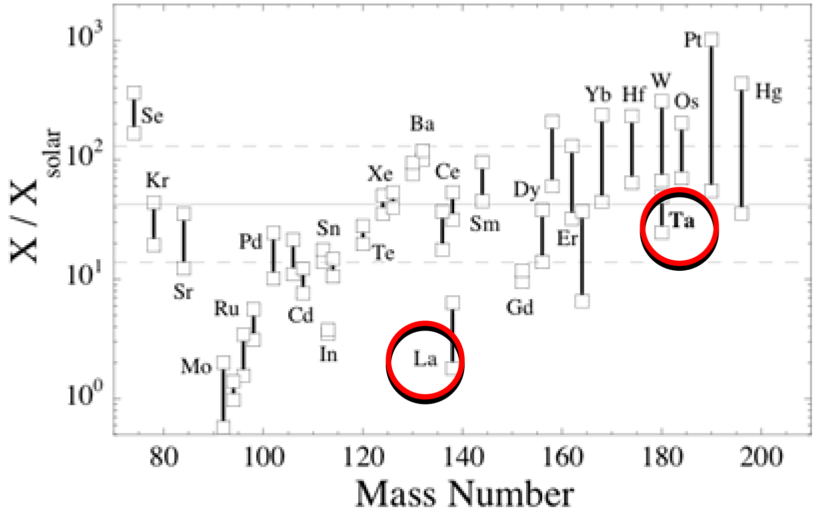

H. Utsunomiya et al., PRC67, 015807 (2003)

Day 1 Experiment #1

^{180}Ta(γ,n) & ^{138}La(γ,n) measurement

20 ^{3}He proportional counters
embedded in polyethylene moderator
Triple-ring configuration

- 1st ring of 4 counters
- 2nd ring of 8 counters
- 3rd ring of 8 counters

4π Neutron Detector

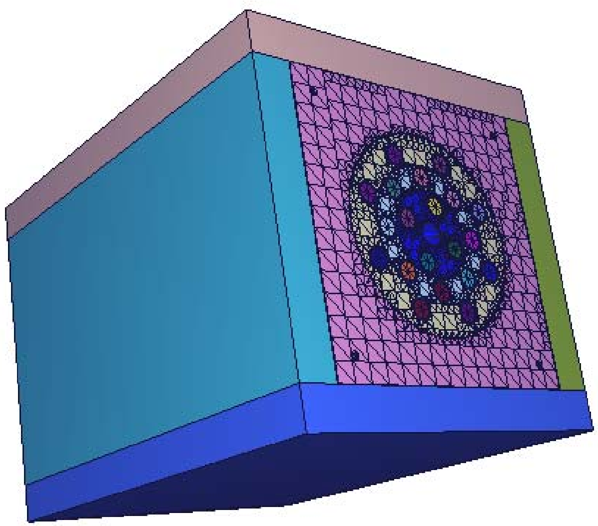

Resonances above S_n

Threshold Photoneutron Technique
Bremsstrahlung + n-TOF

C.D. Berman et al., PRL25, 1302 (1970)
R.J. Baglan et al., PRC3, 2475 (1971)

$^{207}Pb(\gamma,n)$

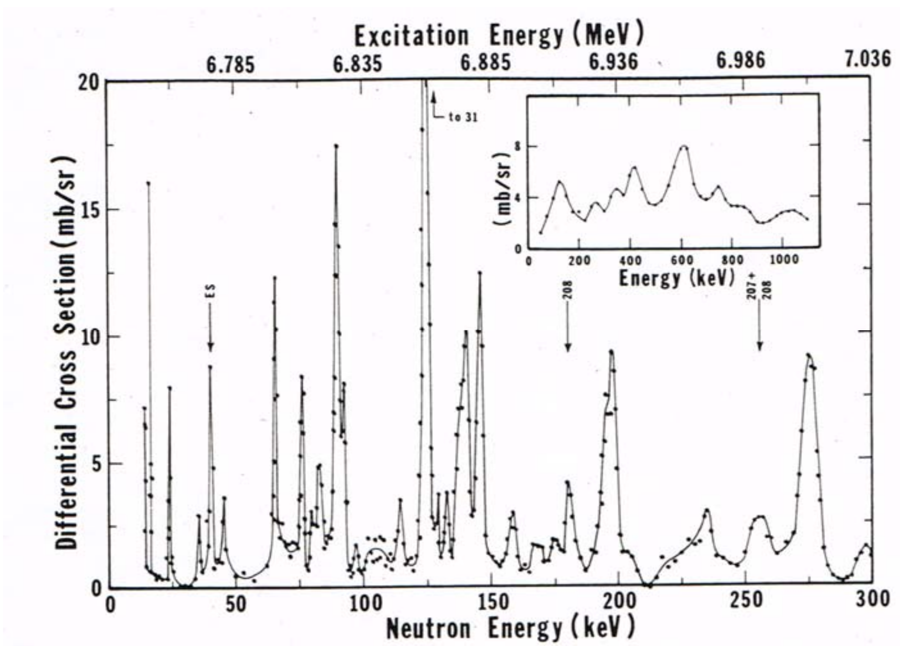

$^{208}Pb(\gamma,n)$

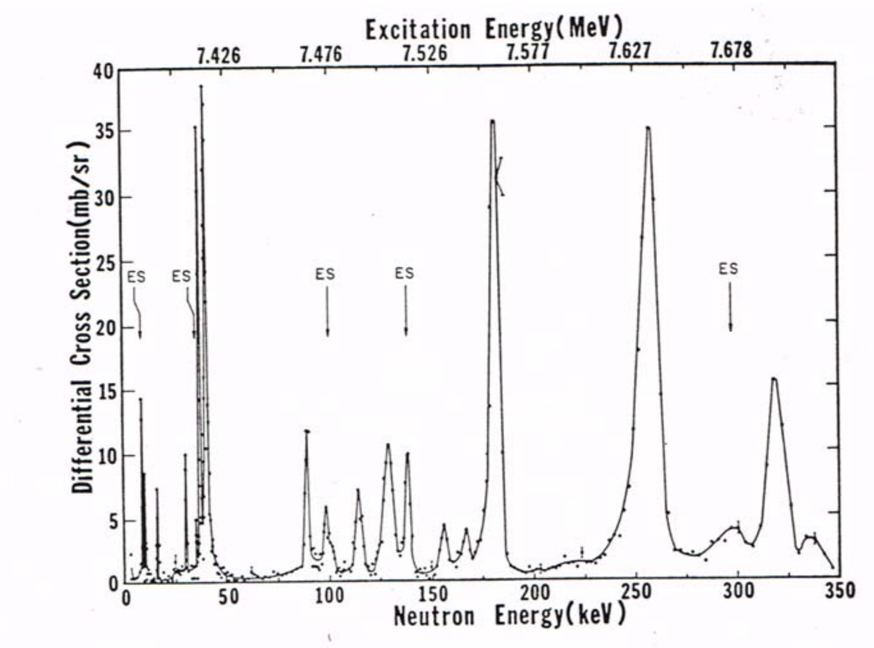

Day 1 Experiment #2

PDR and M1 resonance in ^{207}Pb

- $^{207}Pb(\gamma,n)$ measurement -

Liquid Scintillation and $LaBr_3(Ce)$ Detector Array

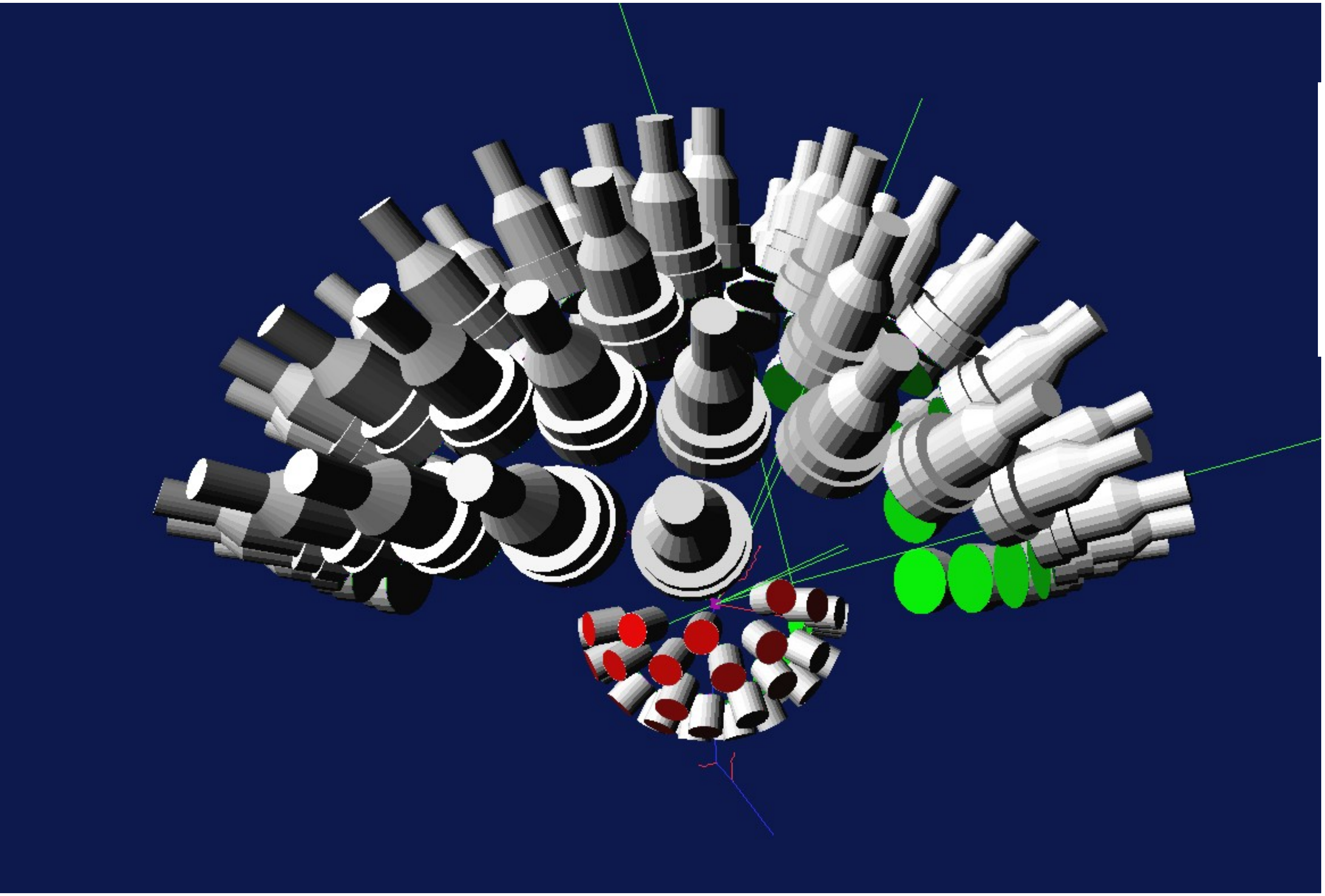

62

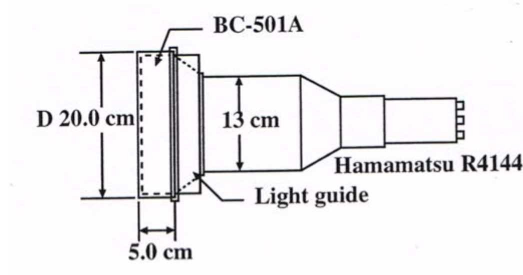

34

$LaBr_3(Ce)$, 3” x 3”

Day 1 Experiment #3

Exclusive neutron decays of GDR in ^{159}Tb

in collaboration with Vladimir Varlamov

- **^{159}Tb(γ,xn) x= 1, 2, 1g/cm^2**
- S_n = 8.133 MeV
- S_{2n} = 14.911 MeV

IAEA –TECDOC-1178

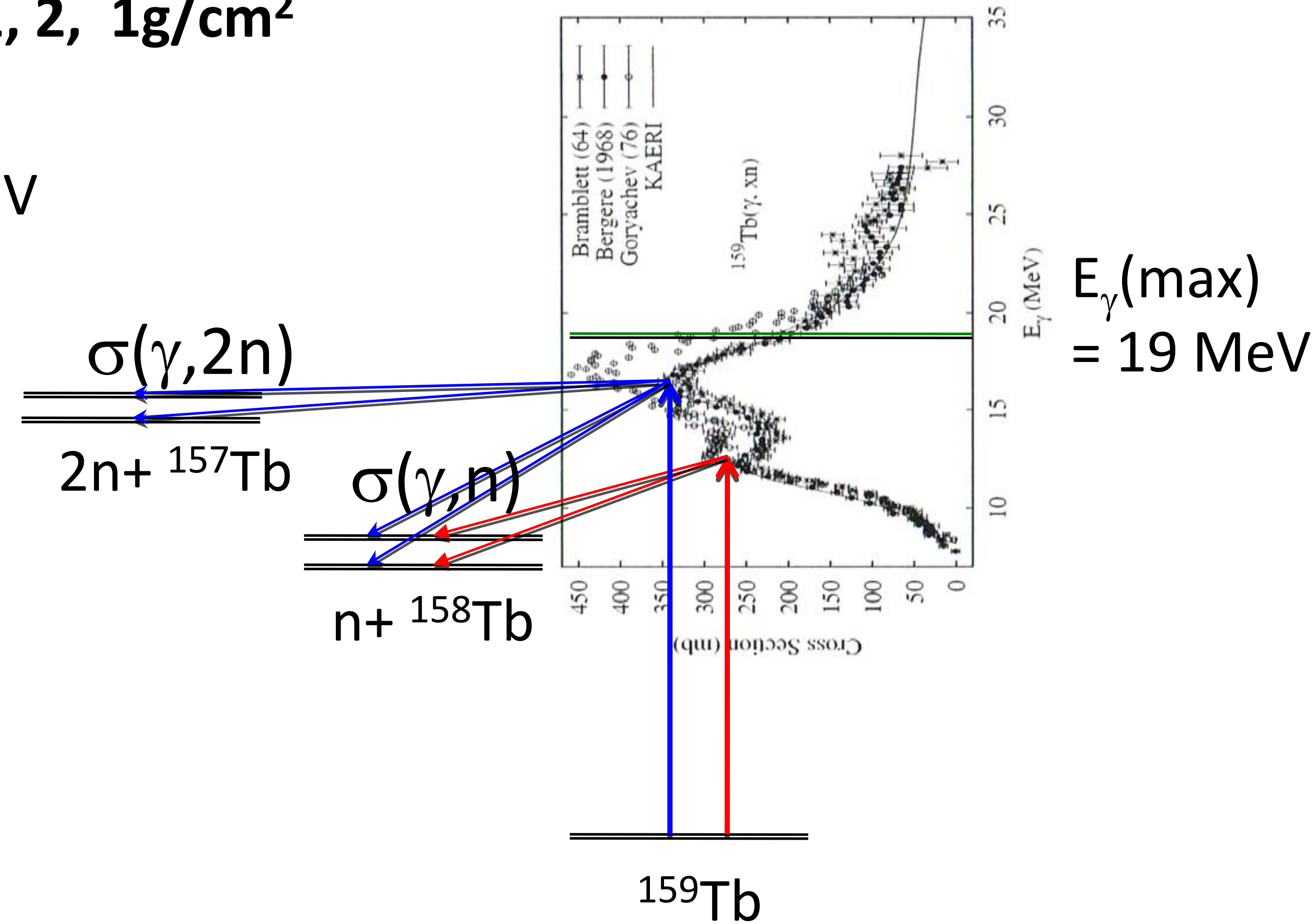

Summary

Personal view of the photonuclear reaction study

- Photonuclear reactions had a glorious days in 1950 through 1980 in the study of GDR with the γ-ray source of positron annihilation in flight. Then, they have slowly faded away toward 1990.
- Photonuclear reactions have revised with the new γ-ray source of laser inverse Compton scattering in the context of nuclear astrophysics at the turn of the 21^{st} century.
- ELI-NP will open up a new era of photonuclear reactions in nuclear science with intense laser and γ-ray beams.